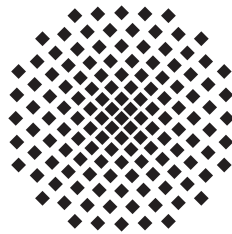# A Quantum-Thermodynamic Approach to Transport Phenomena

Diplomarbeit von
Hendrik Weimer

02.07.2007

Hauptberichter: Prof. Dr. Günter Mahler
Mitberichter: Prof. Dr. Udo Seifert

1. Institut für Theoretische Physik
Universität Stuttgart
Pfaffenwaldring 57, 70550 Stuttgart

Ehrenwörtliche Erklärung

Ich erkläre, dass ich diese Arbeit selbständig verfasst und keine anderen als die angegebenen Quellen und Hilfsmittel benutzt habe.

Stuttgart, 02.07.2007   *Hendrik Weimer*

iv

Contents

Contents

1. Introduction

Advances in miniaturization have been an important driving force for technological progress during the last decades. Transistors on computer chips are getting smaller and smaller, new materials and medical treatments based on nanotechnology have become available, and it seems that there is no end in sight. However, there are fundamental physical constraints on how far this miniaturization process may go. For example, computational building blocks cannot be smaller than the size of an atom, information cannot be transmitted using less than a photon.

In this realm, every physical phenomenon has to be described by quantum mechanics. While the theory has been around now for many decades and has passed all experimental tests so far, there are still many open problems. The greatest challenge in quantum mechanics is the fact that computational problems usually require exponentially more time when incrasing the number of subsystems within a quantum object.

This situation is somewhat akin to the situation in physics before the advent of powerful computers. Already in the 19$^{\text{th}}$ century physicists began to tackle systems consisting of 10^{23} particles, by giving up the desire to track each individual particle, but instead aiming for a holistic description. This led to the highly successful theory of classical thermodynamics.

Recently, thermodynamic concepts have been found to be valid for certain classes of quantum systems [Gemmer04]. Using similar ideas, it might be possible to describe the essential properties of other systems as well, especially far out of equilibrium.

This thesis presents a view on transport phenomena based on the concepts developed in quantum thermodynamics. In this thesis, the term "transport" shall not only refer to transport in the thermodynamic sense concerning quantities like work and heat, but also to transport of information (or lack thereof) and similar concepts. Being a non-equilibrium property by definition, transport behavior is fundamental for characterizing dynamical properties of a system, e.g., when transmitting information or calculating the efficiency of an engine.

Following this introduction and after a discussion of some basic concepts, new definitions for work and heat in quantum systems are presented in chapter 3. Chapter 4 contains an analysis of heat transport in a class of magnetic systems. Subsequently, a novel procedure for temperature control of an atomic system is presented, which is based on the properties of entropy transport in cavity quantum electrodynamics.

1. Introduction

2. Basic Concepts

2.1. Quantum Mechanics

2.1.1. Postulates

The fundamental postulates of quantum mechanics are (see e.g [Cohen-Tannoudji77; Ballentine98])

1. The pure state of a system $|\psi\rangle$ is represented by a complex Hilbert space vector with unit norm.

2. The Hilbert space of a composite system is the tensor product of the Hilbert spaces of the component systems, with operators acting on only one subsystem not affecting the other.

3. Observable quantities are described by Hermitian operators.

4. Changes in the state with respect to time are generated by the operator corresponding to the total energy of a system, changes in position of a particle are generated by the operator corresponding to its momentum.

These four postulates are all that is required to generate a consistent theory with a rich variety of amazing phenomena, which revolutionized 20th-century physics.

2.1.2. Dynamics

The first postulate mandates the dynamics of a quantum system to be norm-preserving. Therefore, it has to be represented by a unitary operator. We then may write

$$|\psi(t + \Delta t)\rangle = \hat{U}(t, \Delta t)|\psi(t)\rangle. \tag{2.1}$$

Using a theorem on one-parameter unitary groups (cf. [Blank94]), there exists an infinitesimal generator $\hat{H}$ such that

$$\hat{U}(t, \Delta t) = \hat{1} - \frac{\mathrm{i}}{\hbar}\hat{H}(t)\Delta t + O(\Delta t^2). \tag{2.2}$$

The fourth postulate tells us that the operator $\hat{H}$ corresponds to the energy of the system. The constant $\hbar$ defines the relation of the energy and time scales. In the following, it will be set to one. Inserting (2.2) into (2.1) brings us to

$$|\psi(t + \Delta t)\rangle = (\hat{1} - \mathrm{i}\hat{H}\Delta t)|\psi(t)\rangle + O(\Delta t^2). \tag{2.3}$$

Performing the limit $\Delta t \to 0$ results in

$$i\frac{\mathrm{d}}{\mathrm{d}t}|\psi(t)\rangle = \hat{H}|\psi(t)\rangle, \tag{2.4}$$

the famous Schrödinger equation.

2.1.3. Interaction picture

For systems involving a Hamiltonian consisting of a time-independent $\hat{H}_0$ and a time-dependent part $\hat{V}(t)$

$$\hat{H} = \hat{H}_0 + \hat{V}(t), \tag{2.5}$$

the dynamics can be simplified if the eigensystem of $\hat{H}_0$ is known. We then may introduce the state in the interaction picture as

$$|\psi_I(t)\rangle = e^{i\hat{H}_0 t}|\psi(t)\rangle. \tag{2.6}$$

Solving for $|\psi(t)\rangle$ and plugging the result into the Schrödinger equation (2.4) leads to

$$i\frac{\mathrm{d}}{\mathrm{d}t}|\psi_I(t)\rangle = \hat{V}_I(t)|\psi_I(t)\rangle, \tag{2.7}$$

with

$$\hat{V}_I(t) = e^{i\hat{H}_0 t}\hat{V}(t)e^{-i\hat{H}_0 t}. \tag{2.8}$$

2.1.4. Coordinate representation

Analogous to Sec. 2.1.2 it is possible to derive the coordinate representation of quantum mechanics from the fourth postulate, resulting in

$$-i\frac{\partial}{\partial x}|\psi(x,t)\rangle = \hat{p}|\psi(x,t)\rangle. \tag{2.9}$$

Therefore, in the coordinate representation the momentum operator $\hat{p}$ takes the form

$$\hat{p} = -i\frac{\partial}{\partial x}. \tag{2.10}$$

This leads to the canonical commutator relation

$$[\hat{x}, \hat{p}]|\psi\rangle = i|\psi\rangle. \tag{2.11}$$

.

2.1.5. Statistical properties

We consider a state

$$|\psi\rangle = \sum c_i |i\rangle. \tag{2.12}$$

Using the tensor product structure established in the second postulate it is possible to derive the following properties of $|\psi\rangle$ (cf. [Zurek05])

- Measuring the state of a quantum system is a statistical process, with different probabilities for different outcomes.

- The probability p_i to find $|\psi\rangle$ in the state $|i\rangle$ is given by

$$p_i = |c_i|^2, \tag{2.13}$$

which is known as Born's rule.

We now look at the statistical properties of an observable O, which according to the second postulate is represented by a Hermitian operator $\hat{O}$. Working in the eigenbasis of $\hat{O}$, we look at the quantity

$$\langle\psi|\hat{O}|\psi\rangle = \sum_{ijk}\langle i|c_i O_k|k\rangle\langle k|c_j|j\rangle = \sum_k p_k O_k. \tag{2.14}$$

Therefore, $\langle\psi|\hat{O}|\psi\rangle$ is the expectation value of O. Another consequence is that the possible outcomes of a measurement of an observable are the eigenvalues of its corresponding operator.

2.1.6. Density operator

In many cases one does not have pure states, but a statistical mixture of pure states, typically due to the system being entangled with the outside world. We therefore introduce the density operator

$$\hat{\rho} = \sum_i p_i |\psi_i\rangle\langle\psi_i|, \tag{2.15}$$

where p_i is the probability to find the system in the pure state $|\psi_i\rangle$. $\hat{\rho}$ is a semi-positive operator with unit trace. The dynamics of $\hat{\rho}$ can be calculated by inserting the Schrödinger equation (2.4) into the time-derivative of (2.15), resulting in

$$\frac{\mathrm{d}}{\mathrm{d}t}\hat{\rho} = -\mathrm{i}[\hat{H}, \hat{\rho}]. \tag{2.16}$$

The properties of a single subsystem of a composite Hilbert space are given by the reduced density matrix

$$\hat{\rho}_1 = \mathrm{Tr}_2\{\hat{\rho}\} = \sum_{i,i'}\sum_j \langle ij|\hat{\rho}|i'j\rangle|i\rangle\langle i'|, \tag{2.17}$$

where $\hat{\rho}_1$ is the reduced density matrix for subsystem 1. The sum over i and i' runs over states in the Hilbert space associated with subsystem 1, while the sum over j is associated with the Hilbert space of subsystem 2.

An important quantity is the purity of a system

$$P = \text{Tr}\left\{\hat{\rho}^2\right\}. \tag{2.18}$$

For pure states, P is always one, whereas for the maximally mixed state of dimension n,

$$\hat{\rho}^{\text{max}} = \frac{1}{n}\hat{1} \tag{2.19}$$

P is at its minimal value, which is $P^{\text{min}} = 1/n$.

A concept similar to the purity is the von Neumann entropy, which is defined as

$$S = -\text{Tr}\left\{\hat{\rho}\log\hat{\rho}\right\}. \tag{2.20}$$

For diagonal states the von Neumann entropy is equal to the Shannon entropy. An important theorem by Araki and Lieb [Araki70] is the triangle inequality

$$|S(\hat{\rho}_1) - S(\hat{\rho}_2)| \leq S(\hat{\rho}) \leq S(\hat{\rho}_1) + S(\hat{\rho}_2). \tag{2.21}$$

This implies that if the total system is pure (i.e., $S(\hat{\rho}) = 0$) the reduced entropies are equal, no matter how the partition into subsystems is performed. On the other hand, if $S(\hat{\rho}_1) = S(\hat{\rho}_2) > 0$ the total state cannot be written as a product state of the two subsystems. This is due to the entanglement between both subsystems, which contributes to the local entropies.

2.1.7. Harmonic oscillator

The Hamiltonian of the one-dimensional harmonic oscillator is given by

$$\hat{H} = \frac{\hat{p}^2}{2m} + \frac{m}{2}\omega^2\hat{x}^2, \tag{2.22}$$

with m being the mass and ω is the eigenfrequency. Using the operators

$$\hat{a} = \sqrt{\frac{m\omega}{2}}\left(\hat{x} + \frac{i}{m\omega}\hat{p}\right) \tag{2.23}$$

$$\hat{a}^\dagger = \sqrt{\frac{m\omega}{2}}\left(\hat{x} - \frac{i}{m\omega}\hat{p}\right) \tag{2.24}$$

the Hamiltonian can be written in the simple form

$$\hat{H} = \omega\left(\hat{a}^\dagger\hat{a} + \frac{1}{2}\right). \tag{2.25}$$

The eigenstates of $\hat{n} = \hat{a}^\dagger \hat{a}$ form a basis in which each basis vector $|n\rangle$ denotes the number of excitations of energy ω stored in the oscillator. The basis $|n\rangle$ is often referred to as the "Fock basis". Since

$$\hat{a}^\dagger |n\rangle = \sqrt{n+1}|n+1\rangle \tag{2.26}$$

$$\hat{a}|n\rangle = \sqrt{n}|n-1\rangle, \tag{2.27}$$

the operators $\hat{a}^\dagger$ and $\hat{a}$ are called creation and annihilation operator, respectively. One further important property is the commutator relation

$$[\hat{a}, \hat{a}^\dagger] = \hat{1}. \tag{2.28}$$

Of particular interest are the eigenstates of the annihilation operator, i.e. solutions to the eigenvalue equation

$$\hat{a}|\alpha\rangle = \alpha|\alpha\rangle. \tag{2.29}$$

In the Fock basis $|\alpha\rangle$ is given by

$$|\alpha\rangle = e^{-|\alpha|^2/2} \sum_n \frac{\alpha^n}{\sqrt{n!}}|n\rangle. \tag{2.30}$$

It is easy to check that these states give rise to a Poisson distribution, i.e.

$$p_n = e^{-|\alpha|^2} \frac{|\alpha|^{2n}}{n!}, \tag{2.31}$$

having the properties

$$\langle n \rangle = |\alpha|^2 \tag{2.32}$$

$$\langle n^2 \rangle - \langle n \rangle^2 = |\alpha|^2. \tag{2.33}$$

In coordinate representation $|\alpha\rangle$ is always a Gaussian wave-packet, which is known to have the minimum uncertainty product $\Delta x \Delta p$. Furthermore, the uncertainty product does not change in time, therefore these states are named "coherent states". Another noteworthy property is that both the mean of position and of momentum evolves according to the solution of the classical harmonic oscillator.

2.1.8. Special operators

In any finite and discrete Hilbert space we may introduce a complete set of orthonormal states $|i\rangle$, i.e.,

$$\langle i|j\rangle = \delta_{ij}$$

$$\sum_i |i\rangle\langle i| = \hat{1}. \tag{2.34}$$

Operators may be represented as a linear combination of the transition operators

$$\hat{P}_{ij} = |i\rangle\langle j|. \tag{2.35}$$

For a two-level system it is often useful to express operators in terms of the $SU(2)$ generators, which are the Pauli matrices

$$
\begin{aligned}
\hat{\sigma}_x &= \begin{pmatrix} & 1 \\ 1 & \end{pmatrix} \\
\hat{\sigma}_y &= \begin{pmatrix} & -\mathrm{i} \\ \mathrm{i} & \end{pmatrix} \\
\hat{\sigma}_z &= \begin{pmatrix} 1 & \\ & -1 \end{pmatrix}.
\end{aligned}
\tag{2.36}
$$

Together with the identity matrix they form a complete basis for Hermitian operators. Furthermore, we define for convenience the transition operators

$$
\begin{aligned}
\hat{\sigma}_+ &= \hat{P}_{12} \\
\hat{\sigma}_- &= \hat{P}_{21}.
\end{aligned}
\tag{2.37}
$$

2.2. Classical Thermodynamics

2.2.1. Fundamentals

Many physically relevant systems, both classical and quantum, consist of a large number of particles. Finding the solution of the equations of motion for such systems is typically either uninteresting or computationally unfeasible, or both. Therefore, classical thermodynamics aims to find a description of the system consisting of only a few variables, while still being able to reproduce the essential properties of the system.

There are various ways how classical thermodynamics may be introduced. In the following we use the ergodic hypothesis as the fundamental principle, which states (see, e.g., [Schwabl00])

> "For an isolated system $\mathcal{S}$ any microstate α compatible with external constraints such as energy or volume is equally probable."

For a system having Ω accessible microstates we introduce the entropy

$$
S = k_B \log \Omega.
\tag{2.38}
$$

Again, the constant k_B defines only a relation between measurement scales and thus will be set to one in the following. An important property is that for isolated systems, S is at its maximum value compatible with external constraints.

2.2.2. Temperature and the Boltzmann distribution

Suppose we have two subsystems $\mathcal{S}_1$ and $\mathcal{S}_2$ being in contact in such a way that only energy may be exchanged. The total energy E is taken to be the sum of the energies of the subsystems

$$
E = E_1 + E_2.
\tag{2.39}
$$

Using the fundamental principle the entropy is given by

$$S(E) \approx S_1(E_1) + S_2(E - E_1), \tag{2.40}$$

which means that the entropy is an additive quantity. Differentiation with respect to E_1 yields

$$\frac{\partial}{\partial E_1} \left[S_1(E_1) + S_2(E - E_1) \right] = 0, \tag{2.41}$$

since $S(E)$ does not depend on E_1. This may be rewritten as

$$\frac{\partial S_1}{\partial E_1} = \frac{\partial S_2}{\partial E_2}. \tag{2.42}$$

Therefore, there exists a quantity that is equal in both subsystems, which we define as the inverse temperature β. One can perform the same calculation for a system where both energy and volume can be exchanged, finally resulting in

$$\frac{\partial S_1}{\partial V_1} = \frac{\partial S_2}{\partial V_2} \equiv \beta p, \tag{2.43}$$

with p being the pressure.

If $\mathcal{S}_2$ is much larger than $\mathcal{S}_1$, we can derive an explicit formula for the probability to find $\mathcal{S}_1$ in a microstate α. We consider

$$p_\alpha = \frac{\Omega_2(E_2)}{\Omega_{tot}(E)} = \frac{e^{S_2(E - E_\alpha)}}{\Omega_{tot}(E)}, \tag{2.44}$$

with E_α being the local energy of the microstate α. Performing a Taylor expansion of $S_2(E - E_\alpha)$ in E_α gives

$$S_2(E - E_\alpha) \approx S_2(E) - \beta E_\alpha, \tag{2.45}$$

finally leading to the Boltzmann distribution

$$p_\alpha = Z^{-1} e^{-\beta E_\alpha}. \tag{2.46}$$

The partition function Z can be obtained due to the p_α being normalized, resulting in

$$Z = \sum_\alpha e^{-\beta E_\alpha}. \tag{2.47}$$

2.2.3. The laws of thermodynamics

We now consider a system with an energy E and a volume V. The complete differential of the entropy $S(E, V)$ is given by

$$dS = \frac{\partial S}{\partial E} dE + \frac{\partial S}{\partial V} dV = \frac{1}{T} dE + \frac{p}{T} dV, \tag{2.48}$$

with $T = \beta^{-1}$. Solving for dE is possible since the entropy is a monotonic function of the temperature, resulting in

$$dE = TdS - pdV. \tag{2.49}$$

If we want to write dE in terms of work and heat energy conservation mandates

$$dE = đQ + đW, \tag{2.50}$$

which is the first law of thermodynamics. Here, the symbol đ denotes that these quantities are not complete differentials. The identification

$$\begin{aligned} đQ &= TdS \\ đW &= -pdV \end{aligned} \tag{2.51}$$

depends on how the changes in work and heat are performed, i.e., on the details of the underlying thermodynamic process. For reversible processes (2.51) is valid.

We now consider a system under some external constraints $\mathbf{X}$, Y. If we remove the constraint Y the system will eventually reach a new macrostate compatible with the new set of constraints. The initial entropy

$$S_i = S(E, \mathbf{X}, Y) \tag{2.52}$$

and the final entropy

$$S_f = S(E, \mathbf{X}) \tag{2.53}$$

will not be the same in general, which may be expressed by recalling that the entropy is at its maximum value compatible with the constraints. This leads to

$$\Delta S = S_f - S_i \geq 0, \tag{2.54}$$

which is the second law of thermodynamics. In a nutshell, it says that for every system the removal of a constraint will never decrease entropy.

2.3. Emergence of Thermodynamics within Quantum Systems

As seen in the previous sections, both quantum mechanics and thermodynamics are theories with statistical properties. However, the main difference is that in quantum mechanics the probabilities play a fundamental role, whereas in thermodynamics the probabilities should emerge from an underlying microscopic theory. As the derivation of thermodynamics from purely classical mechanics has proven to be unsatisfactory, and quantum mechanics already features statistical properties, which classical mechanics is lacking, it is tempting to view thermodynamics as a theory emerging from quantum mechanics under some circumstances. However, it is far less clear in which situations this is possible, that is, when and how quantum and thermodynamic probabilities become equal.
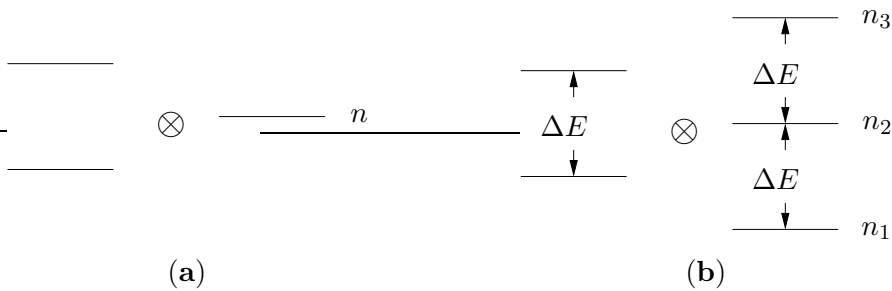
Figure 2.1.: Typical scenarios a two-level system coupled to an environment under microcanonical (**a**) and canonical (**b**) conditions. The n_i denote the degeneracy of the levels.

2.3.1. Basic idea

The main problem for thermodynamic behavior in quantum systems is that of irreversibility. Irreversible dynamics is necessary as thermodynamic systems always relax towards an equilibrium state and stay there for all times. It is obvious that the Schrödinger equation cannot account for irreversible behavior as it is invariant under time-reversal. However, since the Schrödinger equation describes the dynamics of the full system, it is still possible that the dynamics within a subsystem is indeed irreversible [Gemmer04].

It seems natural to partition the whole system into the system proper and the environment. Thus the total Hamiltonian may be written as

$$\hat{H} = \hat{H}_S + \hat{H}_E + \hat{H}_{SE}, \tag{2.55}$$

where $\hat{H}_S$ acts only on the system, $\hat{H}_E$ acts only on the environment and $\hat{H}_{SE}$ contains the interaction between system and environment. In order to actually be able to speak of an environment, its Hilbert space must be sufficiently larger than the Hilbert space of the system. The structure of $\hat{H}_{SE}$ determines what type of environment is realized, e.g., microcanonical (no energy exchange allowed) or canonical (energy change allowed) conditions. Typical model systems are depicted in Fig. 2.1.

2.3.2. Observations

By introducing a probability measure for the total Hilbert space one can show that the local purity of a gas-container system under microcanonical conditions [Fig. 2.1(**a**)] is at its maximum, thus proving the second law [Gemmer01b]. Furthermore, under canonical coupling [Fig. 2.1(**b**)] the system will be Boltzmann distributed (2.46), provided that the degeneracy in the environment grows exponentially [Gemmer03], i.e,

$$n_i \propto e^{\beta E_i}. \tag{2.56}$$

Here, E_i is the energy of the level i and β is the spectral temperature of the container. While the system will be in a canonical state with temperature β, the environment will typically be in a non-thermal state [Borowski03].

3. Work and Heat in Quantum Systems

The formulation of classical thermodynamics was one of the most important achievements of the 19th century, as it allowed to investigate a large variety of phenomena, including the workings of thermodynamical machines. The first law of thermodynamics,

$$\mathrm{d}U = \text{đ}W + \text{đ}Q, \tag{3.1}$$

combined with definitions for the infinitesimal change in work đW and heat đQ and the second law is all that is required for computing important quantities like the efficiency of a process.

In the quantum realm, the classification of work and heat is less clear. So far, it has been mainly derived from the change of the total energy expectation value

$$\mathrm{d}U = \mathrm{d}\mathrm{Tr}\left\{\hat{H}\hat{\rho}\right\} = \mathrm{Tr}\left\{\hat{\rho}\mathrm{d}\hat{H} + \hat{H}\mathrm{d}\hat{\rho}\right\}, \tag{3.2}$$

and defining the first term as đW and the second as đQ [Alicki79; Kosloff84; Kieu04; Henrich06]. However, such a classification is problematic, as can be seen in a simple example. Consider the Hamiltonian

$$\hat{H} = \frac{\Delta E}{2}\hat{\sigma}_z + g\hat{\sigma}_x, \tag{3.3}$$

where $\hat{\sigma}_z$ describes the original energy eigenbasis of a system and $g\hat{\sigma}_x$ is an external time-independent driving force. According to (3.2) there is obviously no work performed on the system. However, if we look at the time-evolution of a system initially in its ground state, the probability to find it in the excited state is given by

$$p_e(t) = 2g^2 \frac{1 - \cos\left(\sqrt{\Delta E^2 + 4g^2}\, t\right)}{\Delta E^2 + 4g^2} \tag{3.4}$$

As shown in Fig. 3.1 this may even lead to inversion in the system, hinting at the possibility to extract work from the system. While in some cases this problem may be fixed by regarding only processes in which the fields are switched on and off, the microscopic foundation of Eq. (3.2) is rather unclear.

Nevertheless thermodynamic behavior may occur even in small quantum systems [Gemmer04], so in principle it should be possible to obtain đW and đQ even there. In the following, we will present a definition that does not suffer from the problems above.

This chapter is organized as follows. We first discuss the effective local dynamics of a bipartite quantum system. Based upon what an experimentalist would observe, we
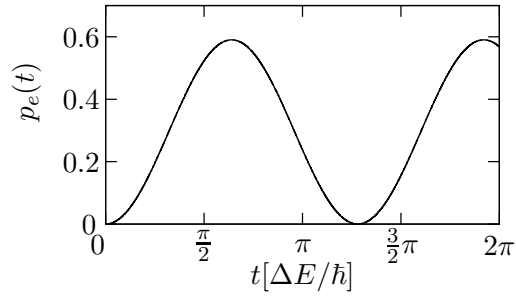
Figure 3.1.: Probability to find a system driven by a time-independent Hamiltonian in the excited state of the original eigenbasis. ($\Delta E = 1$, $g = 0.6$)

give a definition for the local energy. We then show that the change in local energy can always be split into a part that coincides with a change in entropy and in a part which does not. Corresponding to classical thermodynamics, the former is called "heat" and the latter is called "work". Our definitions for the local heat and work do not only depend on local properties, but on properties of the whole system. We explicitly give formulas to calculate the non-local quantities once the time evolution of the full system is known. Finally, some examples will be given.

3.1. The LEMBAS principle [Weimer07]

We consider an autonomous bipartite system described by the Hamiltonian

$$\hat{H} = \hat{H}_A + \hat{H}_B + \hat{H}_{AB}, \tag{3.5}$$

where $\hat{H}_A$ acts only on subsystem A and $\hat{H}_B$ only on B, respectively. In agreement with the results from classical thermodynamics, we define the infinitesimal work đW performed on A as the change in its internal energy dU that does not change its local von Neumann entropy, i.e.

$$\mathrm{d}S = 0 \Leftrightarrow \mathrm{d}W = \mathrm{d}U. \tag{3.6}$$

The remainder is defined as the infinitesimal heat đQ.

The dynamics of the subsystem A is given by the Liouville-von Neumann equation

$$\frac{\partial}{\partial t}\hat{\rho}_A = -\mathrm{i}[\hat{H}_A + \hat{H}^{\mathrm{eff}}, \hat{\rho}_A] + \mathcal{L}_{inc}(\hat{\rho}), \tag{3.7}$$

where $\hat{\rho}_A$ is the reduced density operator of A, $\hat{H}^{\mathrm{eff}}$ is an effective Hamiltonian describing the unitary dynamics induced by B and $\mathcal{L}_{\mathrm{inc}}$ is a superoperator describing incoherent processes. Since $\mathcal{L}_{\mathrm{inc}}$ is a function of the density operator of the full system, eqn. (3.7) is not necessarily a closed differential equation.

We now consider a hypothetical measurement of the local effective energy in A. One could imagine an experimentalist tuning a laser over the whole spectrum and recording the absorption profile. However, depending on the angle and the polarization of the laser

beam, a different spectrum will be observed. Thus the experimentalist introduces a local effective measurement basis (LEMBAS). In the following we study how this concept can be incorporated into the derivation of work and heat. It is important to note that this results in work and heat depending on the measurement basis chosen, i.e., they are basis-dependent quantities.

If one choses the energy basis of subsystem A as the measurement basis, only the parts of the total effective Hamiltonian $\hat{H}^{\text{eff}}$ that commute with $\hat{H}_A$ will affect measurements of the type described above. To find this part $\hat{H}_1^{\text{eff}}$, we expand $\hat{H}^{\text{eff}}$ in the transition operator basis defined by the energy eigenstates $\{|j\rangle\}$:

$$\hat{H}^{\text{eff}} = \sum_{jk} (\hat{H}^{\text{eff}})_{jk} |j\rangle\langle k| \tag{3.8}$$

Using this operator basis, we have

$$\left[\hat{H}_A, |j\rangle\langle k|\right] = \omega_{jk} |j\rangle\langle k|, \tag{3.9}$$

where ω_{jk} is the difference between the energy eigenvalues of the states $|j\rangle$ and $|k\rangle$, and therefore $\omega_{jj} = 0$ for non-degenerate energy eigenvalues. Now, we define

$$\hat{H}_1^{\text{eff}} = \sum_{j} (\hat{H}^{\text{eff}})_{jj} |j\rangle\langle j| \tag{3.10}$$

which is the diagonal part of $\hat{H}^{\text{eff}}$. From Eq. (3.9), we see that no non-trivial linear combination of transition operators $|j\rangle\langle k|$ commutes with $\hat{H}_A$. Therefore, the remaining part $\hat{H}_2^{\text{eff}} = \hat{H}^{\text{eff}} - \hat{H}_1^{\text{eff}}$ does not commute with $\hat{H}_A$, resulting in

$$[\hat{H}_1^{\text{eff}}, \hat{H}_A] = 0, \ [\hat{H}_2^{\text{eff}}, \hat{H}_A] \neq 0, \tag{3.11}$$

except for the case where $\hat{H}_2^{\text{eff}} = 0$.

3.2. Definitions for work and heat

If a measurement of the local energy is performed in the energy eigenbasis of $\hat{H}_A$, the corresponding operator is

$$\hat{H}' = \hat{H}_A + \hat{H}_1^{\text{eff}}. \tag{3.12}$$

Therefore, the change in internal energy within A is given by

$$dU = \frac{d}{dt} \text{Tr}\left\{\hat{H}'\hat{\rho}_A\right\} dt = \text{Tr}\left\{\dot{\hat{H}}'\hat{\rho}_A + \hat{H}'\dot{\hat{\rho}}_A\right\} dt. \tag{3.13}$$

Using (3.7) and $\hat{H}_A$ being time-independent leads to

$$dU = \text{Tr}\left\{\dot{\hat{H}}_1^{\text{eff}}\hat{\rho}_A - i[\hat{H}', \hat{H}_2^{\text{eff}}]\hat{\rho}_A + \hat{H}'\mathcal{L}_{\text{inc}}(\hat{\rho})\right\} dt, \tag{3.14}$$

15

where the cyclicity of the trace has been used. Observing that the dynamics induced by the first two terms is unitary, we arrive at

$$\text{d}W \quad = \quad \text{Tr}\left\{\dot{\hat{H}}_1^{\text{eff}}\hat{\rho}_A - \text{i}[\hat{H}', \hat{H}_2^{\text{eff}}]\hat{\rho}_A\right\}\text{d}t \tag{3.15}$$

$$\text{d}Q \quad = \quad \text{Tr}\left\{\hat{H}'\mathcal{L}_{\text{inc}}(\hat{\rho})\right\}\text{d}t. \tag{3.16}$$

Following this approach, it is possible to define heat and work for any quantum mechanical process, regardless of the type of dynamics or the states involved.

In order to actually compute $\text{d}W$ and $\text{d}Q$, the effective Hamiltonian $\hat{H}^{\text{eff}}$ is required. By starting with the Liouville-von Neumann equation for the full system

$$\frac{\partial}{\partial t}\hat{\rho} = -\text{i}[\hat{H}, \hat{\rho}] \tag{3.17}$$

and taking the partial trace over B [cf. (2.17)] yields

$$\frac{\partial}{\partial t}\hat{\rho} = \text{Tr}_B\left\{[\hat{H}_A + \hat{H}_B + \hat{H}_{AB}, \hat{\rho}]\right\}. \tag{3.18}$$

Applying some theorems on partial traces (cf. appendix A) shows that terms involving $\hat{H}_B$ vanish, and that $\hat{H}_A$ generates the local dynamics in A. For dealing with the terms involving $\hat{H}_{AB}$, we first split the density operator

$$\hat{\rho} = \hat{\rho}_A \otimes \hat{\rho}_B + \hat{C}_{AB}, \tag{3.19}$$

where $\hat{\rho}_{A,B}$ are the reduced density matrices for A and B, respectively, and $\hat{C}_{AB}$ is the operator describing the correlations between both subsystems. Since the first term represents a factorizing density matrix the factorization approximation is exact, and we can write (cf. [Gemmer01a])

$$\text{Tr}_B\left\{[\hat{H}_{AB}, \hat{\rho}_A \otimes \hat{\rho}_B]\right\} = [\hat{H}^{\text{eff}}, \hat{\rho}], \tag{3.20}$$

where $\hat{H}^{\text{eff}}$ is given by

$$\hat{H}^{\text{eff}} = \text{Tr}_B\left\{\hat{H}_{AB}(\hat{1}_A \otimes \hat{\rho}_B)\right\}. \tag{3.21}$$

We will now show that the processes generated by $[\hat{H}_{AB}, \hat{C}_{AB}]$ cannot result in unitary dynamics, but will always change the local von Neumann entropy S_A. In order to prove this, we compute its time derivative

$$\dot{S}_A = -\text{Tr}\left\{[\hat{H}_{AB}, \hat{C}_{AB}]\log\hat{\rho}_A \otimes \hat{1}_B\right\}. \tag{3.22}$$

Therefore, any dynamics generated by this term cannot be unitary, but results in a contribution to $\mathcal{L}_{\text{inc}}$. If the dynamics of the full system is unitary, we have

$$\mathcal{L}_{\text{inc}} = -\text{i}\text{Tr}_B\left\{[\hat{H}_{AB}, \hat{C}_{AB}]\right\}. \tag{3.23}$$

3.3. Equilibrium properties

An open question remains in how these new definition of heat and work are linked to the common one (3.2). It is easy to check that for $\hat{H}_2^{\text{eff}} = 0$ the definitions are identical. This is the case if we only consider quasistatic processes, where we can investigate the local temperature of, say, system A. From the Gibbs fundamental relation it is known that

$$\mathrm{d}S = \frac{1}{T}\mathrm{d}Q. \tag{3.24}$$

Using now the definition given for the heat in (3.16) we get

$$\mathrm{d}S_A = \frac{1}{T^*}\mathrm{Tr}\left\{\hat{H}'\mathcal{L}_{\text{inc}}(\hat{\rho})\right\}\mathrm{d}t. \tag{3.25}$$

T^* should indicate a parameter associated with the local temperature. On the other side we know the derivation of the entropy S_A from (3.22) combined with (3.25) gives

$$-\mathrm{Tr}\left\{\mathcal{L}_{\text{inc}}(\hat{\rho})\log\hat{\rho}_A\right\} = \frac{1}{T^*}\mathrm{Tr}\left\{\hat{H}'\mathcal{L}_{\text{inc}}(\hat{\rho})\right\}$$
$$T^* = \frac{\mathrm{Tr}\left\{\mathcal{L}_{\text{inc}}(\hat{\rho})\log\hat{\rho}_A\right\}}{\mathrm{Tr}\left\{\hat{H}'\mathcal{L}_{\text{inc}}(\hat{\rho})\right\}}. \tag{3.26}$$

For canonical states $\hat{H}'$ commutes with $\hat{\rho}_A$ and $\mathcal{L}_{\text{inc}}(\hat{\rho}_A)$, thus (3.26) is equivalent to the classical definition

$$T = \frac{\partial U}{\partial S}. \tag{3.27}$$

T^* is not necessarily equal to the global temperature of the full system due to the interaction between the individual systems inducing correlations [Hartmann04a; Hartmann04b].

3.4. Further examples

3.4.1. Detuned laser

Using the LEMBAS principle, it is now possible to investigate work and heat in concrete physical systems. First we consider a two-level atom with a local Hamiltonian $\hat{H}_A$ driven by a laser field $\hat{V}$. In the semiclassical treatment of the radiation field emitted by a laser, the total Hamiltonian is given by

$$\hat{H} = \hat{H}_A + \hat{V} = \frac{\Delta E}{2}\hat{\sigma}_z + g\sin\omega t\hat{\sigma}_x, \tag{3.28}$$

where g is the coupling strength and ω the laser frequency. In the rotating wave approximation the Hamiltonian can be made time-independent. We investigate the situation where the atom is initially in a thermal state described by the density operator

$$\hat{\rho}(0) = Z^{-1}\exp(-\beta\hat{H}_A), \tag{3.29}$$

with Z being the partition function and β the inverse temperature.

In order to calculate $đW$ and $đQ$ we first need to diagonalize the Hamiltonian, which can be made time-independent by applying the unitary transformation

$$\hat{U}_1 = e^{i\omega t}\hat{P}_{11} + \hat{P}_{22}. \tag{3.30}$$

This leads to the time evolution operator

$$\hat{U} = \begin{pmatrix} e^{i(\delta+\Delta E)t/2}\left[\cos\left(\frac{\Omega t}{2}\right) - i\frac{\delta}{\Omega}\sin\left(\frac{\Omega t}{2}\right)\right] & -i\frac{g}{\Omega}e^{i(\delta+\Delta E)t/2}\sin\left(\frac{\Omega t}{2}\right) \\[2ex] -i\frac{g}{\Omega}e^{-i(\delta+\Delta E)t/2}\sin\left(\frac{\Omega t}{2}\right) & e^{-i(\delta+\Delta E)t/2}\left[\cos\left(\frac{\Omega t}{2}\right) + i\frac{\delta}{\Omega}\sin\left(\frac{\Omega t}{2}\right)\right] \end{pmatrix}, \tag{3.31}$$

where $\Omega = \sqrt{g^2 + \delta^2}$ is the Rabi frequency and $\delta = \omega - \Delta E$ is the detuning from the resonance frequency. Since (3.28) is already an effective description we can directly compute $đW$ and $đQ$ resulting in

$$đW = \frac{\Delta E g^2}{2\Omega}\tanh\frac{\beta\Delta E}{2}\sin\Omega t \tag{3.32}$$

$$đQ = 0. \tag{3.33}$$

For comparison, using (3.2) leads to

$$đW = \frac{(\Delta E + \delta)g^2}{2\Omega}\tanh\frac{\beta\Delta E}{2}\sin\Omega t. \tag{3.34}$$

Since the maximum of this expression is not at the resonance frequency (i.e., $\delta = 0$), this result is unphysical.
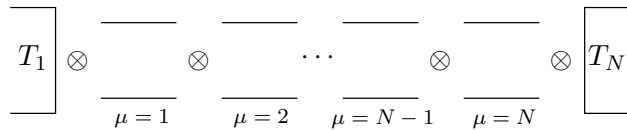
3.4.2. One-dimensional spin chain

Another case in which the LEMBAS principle can be applied is the study of stationary steady states. Consider a linear chain of spins between two baths at different temperatures (Fig. 3.2). The Hamiltonian for the spin chain consists of a local Zeeman splitting and an XXZ interaction, i.e.

$$\hat{H} = \sum_{\mu}^{N}\frac{\Delta E}{2}\hat{\sigma}_z^{(\mu)} + \lambda\left(\hat{\sigma}_x^{(\mu)}\otimes\hat{\sigma}_x^{(\mu+1)} + \hat{\sigma}_y^{(\mu)}\otimes\hat{\sigma}_y^{(\mu+1)} + \delta\hat{\sigma}_z^{(\mu)}\otimes\hat{\sigma}_z^{(\mu+1)}\right). \tag{3.35}$$

The bath coupling is realized by two dissipators $\mathcal{D}_{1,N}$ in Lindblad form (cf. [Michel03]), with

$$\mathcal{D}_i(\hat{\rho}) = W_{10}^{(i)}(2\hat{\sigma}_-^{(i)}\hat{\rho}\hat{\sigma}_+^{(i)} - \hat{\rho}\hat{\sigma}_+^{(i)}\hat{\sigma}_-^{(i)} - \hat{\sigma}_+^{(i)}\hat{\sigma}_-^{(i)}\hat{\rho}) + W_{01}^{(i)}(2\hat{\sigma}_+^{(i)}\hat{\rho}\hat{\sigma}_-^{(i)} - \hat{\rho}\hat{\sigma}_-^{(i)}\hat{\sigma}_+^{(i)} - \hat{\sigma}_-^{(i)}\hat{\sigma}_+^{(i)}\hat{\rho}). \tag{3.36}$$

Figure 3.2.: Linear spin chain coupled to two baths at different temperatures T_1, T_N.
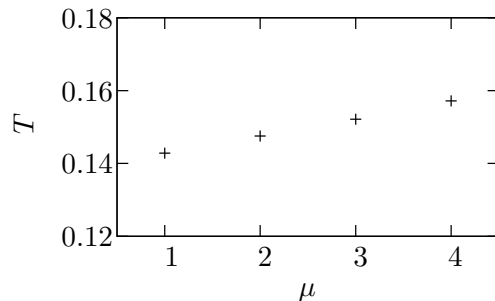
Figure 3.3.: Fourier's law in a Heisenberg chain. ($\Delta E = 1$, $\lambda = \lambda_B = 0.01$, $T_1 = 0.1$, $T_2 = 0.2$)

Such a dissipator correctly describes the effect of a bath as long as the system is homogeneous and the internal coupling is small [Wichterich07]. The rates W_{10} and W_{01} are connected to the bath temperatures by

$$
\begin{aligned}
W_{10}^{(i)} &= \lambda_B(1 - T_i) \\
W_{01}^{(i)} &= \lambda_B T_i.
\end{aligned}
\tag{3.37}
$$

Here, λ_B is the coupling strength of the interaction with the bath.

In a suitable parameter range for a Heisenberg chain ($\delta = 1$) the system has a stationary steady state satisfying Fourier's law, i.e.,

$$
\mathbf{J}_{th} = \kappa \nabla T,
\tag{3.38}
$$

with $\mathbf{J}_{th}$ being the heat current within the system, κ being the thermal conductivity and ∇T the internal temperature gradient [Michel03]. For a system of $N = 4$ spins this is shown in Fig. 3.3. Conversely, as can bee seen in Fig. 3.4, the Förster chain ($\delta = 0$) has a stationary steady state without an internal temperature gradient, i.e., the conductivity is infinite.

Let us now try to find the stationary state for two inner spins. Since in the stationary state the continuity equation for the probabilities reads

$$
\dot{p}_\mu = -\nabla \mathbf{j} = 0,
\tag{3.39}
$$

the reduced density matrix of a single spin, $\hat{\rho}_\mu$, has to be diagonal. Another simplification can be made by using that the Hamiltonian contains only nearest-neighbor interactions. Using theorem A.5 we obtain for the effective Hamiltonian of a single spin

$$
\hat{H}_\mu^{\text{eff}} = \left[\frac{\Delta E}{2} + 2\lambda\delta(p_{\mu-1} + p_{\mu+1} - 1) \right] \hat{\sigma}_z.
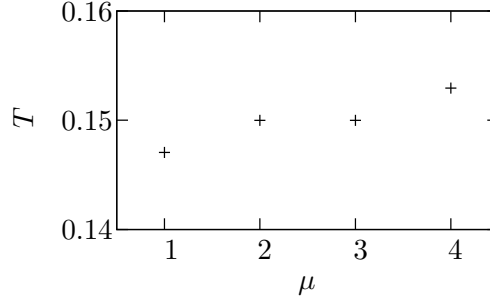\tag{3.40}
$$

19

Figure 3.4.: Temperature profile for a Förster chain. (Same parameters as in Fig. 3.3)

However, it is not sufficient to project out single spins as

$$[\hat{H}_\mu^{\mathrm{eff}}, \hat{\rho}_\mu] = 0, \tag{3.41}$$

i.e., it is not possible to extract information on the relationship between internal currents and gradients this way. Instead we consider the two-spin density operator

$$\hat{\rho}_{\mu,\mu+1} = \begin{pmatrix} c_{\mu,\mu+1} + \bar{p}_\mu \bar{p}_{\mu+1} & 0 & 0 & 0 \\ 0 & \bar{p}_\mu p_{\mu+1} - c_{\mu,\mu+1} & -\frac{J}{4\lambda}(\chi_{\mu,\mu+1} + \mathrm{i}) & 0 \\ 0 & -\frac{J}{4\lambda}(\chi_{\mu,\mu+1} - \mathrm{i}) & \bar{p}_{\mu+1} p_\mu - c_{\mu,\mu+1} & 0 \\ 0 & 0 & 0 & c_{\mu,\mu+1} + p_\mu p_{\mu+1} \end{pmatrix}. \tag{3.42}$$

Here, $c_{\mu,\mu+1}$ are classical correlations, J is the probability current, $\chi_{\mu,\mu+1}$ are off-diagonal elements not contributing to the current, and

$$\bar{p}_\mu = 1 - p_\mu. \tag{3.43}$$

In order to check that the current J is indeed the expectation value of the probability current we use the current operator (cf. [Michel04])

$$\hat{J}_{\mu,\mu+1} = \mathrm{i}\lambda(\hat{\sigma}_+^{(\mu)} \hat{\sigma}_-^{(\mu+1)} - \hat{\sigma}_-^{(\mu)} \hat{\sigma}_+^{(\mu+1)}), \tag{3.44}$$

which has the expectation value

$$\langle J_{\mu,\mu+1} \rangle = \mathrm{Tr}\left\{ \hat{J}_{\mu,\mu+1} \hat{\rho}_{\mu,\mu+1} \right\} = J. \tag{3.45}$$

Let us now concentrate on the first two spins, i.e, $\hat{\rho}_{1,2}$. The local Liouville von Neumann equation reads for the stationary state

$$\frac{\partial}{\partial t}\hat{\rho}_{1,2} = [\hat{H}^{\mathrm{eff}}, \hat{\rho}_{1,2}] + \mathcal{D}_1(\hat{\rho}_{1,2}) + \mathcal{L}_{\mathrm{inc}}^{(2,3)}(\hat{\rho}_{1,2,3}) = 0, \tag{3.46}$$

with $\hat{H}^{\text{eff}}$ being given by

$$\hat{H}^{\text{eff}} = \frac{\Delta E}{2}\hat{\sigma}_z^{(1)} + \left[\frac{\Delta E}{2} + 2\lambda\delta(p_3 - 1)\right]\hat{\sigma}_z^{(2)}. \tag{3.47}$$

and the incoherent term being

$$\mathcal{L}_{\text{inc}}^{(2,3)}(\hat{\rho}_{1,2,3}) = -\text{i}\text{Tr}_3\left\{[\hat{H}_{2,3}, \hat{C}_{123}]\right\}, \tag{3.48}$$

with $\hat{C}_{123}$ being the operator describing the three-particle correlations. While Eq. (3.46) imposes constraints on the stationary state, it does not provide a closed set of equations. Such a set can only be found if all local two-spin density operators are taken into account. However, finding a solution to this set involves solving a large number of non-linear equation and thus is a highly complicated task. Given a solution exists, one has found a set of local variables describing the relevant properties of the system. In this sense the system behaves thermodynamic, as it is not necessary to solve the full Liouville von Neumann equation. Once this set of variables is found one might even be able to tackle long-standing problems like whether or not there exists a principle of mimimum entropy production [Prigogine67] in the quantum realm.

Even without knowing the solution to (3.46) further statements can be made. As the system is homogenous and weakly coupled the external energy current flowing from the baths into the system have to be identical to the internal energy current

$$J_E = J\Delta E. \tag{3.49}$$

The external energy current can be determined by writing down the Liouville von Neumann equation for the full system, multiplying with the system Hamiltonian and taken the trace, i.e,

$$\begin{aligned}
\text{Tr}\left\{\hat{H}\frac{\partial}{\partial t}\hat{\rho}\right\} &= -\text{i}\text{Tr}\left\{[\hat{H}, \hat{H}]\hat{\rho}\right\} + \text{Tr}\left\{\hat{H}\mathcal{D}_1(\hat{\rho})\right\} + \text{Tr}\left\{\hat{H}\mathcal{D}_N(\hat{\rho})\right\} \\
&= \text{Tr}\left\{\hat{H}\mathcal{D}_1(\hat{\rho})\right\} + \text{Tr}\left\{\hat{H}\mathcal{D}_N(\hat{\rho})\right\}.
\end{aligned} \tag{3.50}$$

In the stationary state we thus have

$$J_E = -\text{Tr}\left\{\hat{H}\mathcal{D}_1(\hat{\rho})\right\} = \text{Tr}\left\{\hat{H}\mathcal{D}_N(\hat{\rho})\right\}. \tag{3.51}$$

Performing partial traces over everything but the two spins next to the baths leads to

$$J_E = -\text{Tr}\left\{\hat{H}_{1,2}^{\text{eff}}\mathcal{D}_1(\hat{\rho}_{1,2})\right\} = \text{Tr}\left\{\hat{H}_{1,2}^{\text{eff}}\mathcal{D}_N(\hat{\rho}_{N-1,N})\right\}. \tag{3.52}$$

We further trace over the second-last spin, resulting in

$$J_E = -\text{Tr}\left\{\hat{H}_1^{\text{eff}}\mathcal{D}_1(\hat{\rho}_1)\right\} = \text{Tr}\left\{\hat{H}_1^{\text{eff}}\mathcal{D}_N(\hat{\rho}_N)\right\}. \tag{3.53}$$

Plugging the ansatz (3.42) for $\hat{\rho}_{1,2}$ and (3.36) into (3.52) and (3.53) yields

$$J_E = \frac{\lambda_B}{2}[\chi_{1,2}J - 8c_{1,2}\lambda\delta - 2(p_1 - T_1)(\Delta E - 2\lambda\delta + 4\lambda\delta p_2)] \tag{3.54}$$

$$J_E = \lambda_B(p_1 - T_1)[2\lambda\delta(2p_2 - 1) + \Delta E]. \tag{3.55}$$

For a Förster chain this eventually results in

$$J_E = \lambda_B\Delta E(p_1 - T_1) \tag{3.56}$$

$$\chi_{1,2} = 0, \tag{3.57}$$

and analogously in

$$J_E = \lambda_B\Delta E(p_N - T_N) \tag{3.58}$$

$$\chi_{N-1,N} = 0. \tag{3.59}$$

4. Heat Transport in Magnetic Systems

Quantum magnets, i.e. low-dimensional quantum systems dominated by spin-spin inter-actions, have become a subject of intense investigation in recent years [Schollwöck04]. These systems allow to study a large variety of quantum effects yet are described by rather simple interactions, making them interesting both from an experimental and theoretical point of view. Of particular interest are the heat transport properties of so-called "telephone number compounds", materials containing 1D and 2D spin structures. Experimental observations show extremely large thermal conductivity along spin chains and normal values perpendicular to them [Sologubenko00; Hess01].

A rather large amount of spins will be required before one can reliably characterize the transport behavior; a theoretical approach to heat conductivity from first principles is thus rather complicated. So far the heat transport has primarily been investigated in terms of the Green-Kubo formula [Zotos97; Klümper02; Heidrich-Meisner03; Saito03; Jung06]; the main advantage of this approach is its computability after having diagonalized the system Hamiltonian. Derived on the basis of linear response theory the Kubo formula has originally been formulated for electrical transport [Kubo57; Kubo91]. Basically one is interested in a current-current auto-correlation, which has ad hoc been transfered to heat transport simply by replacing the electrical current by a heat current [Luttinger64]. However, the justification of this replacement remains questionable since there is no way of expressing a temperature gradient in terms of an addend to the Hamiltonian as in electrical transport [Gemmer06].

Other approaches to heat conductivity in quantum systems are based on direct diagonalization of the Schrödinger equation of a limited number of spins [Gobert05], analyzing the level statistics of the Hamiltonian [Mejía-Monasterio05; Steinigeweg06] or by an explicit coupling to some environments of different temperature [Saito03; Michel03]. In the latter case, environments are described by a quantum master equation [Breuer02] in Liouville space. Here the temperature differences can, indeed, be described by a perturbation operator so that one may treat a thermal perturbation in this extended state space similar as an electrical one in the Hilbert space [Michel04].

The so-called Hilbert space Average Method [Gemmer04] allows for a direct investigation of the heat transport in quantum systems from Schrödinger dynamics. By deriving a reduced dynamical equation for a class of design quantum systems, normal heat transport as well as Fourier's law has been confirmed [Michel05; Michel06]. Recently, it has been shown that for diffusive systems the Hilbert space average method is equivalent to a projection operator technique with an extended projection operator [Breuer06; Breuer07]. However, ballistic behavior cannot be analyzed with the Hilbert space Average Method in a straight-forward manner since it is not obvious how to obtain time-dependent rates.
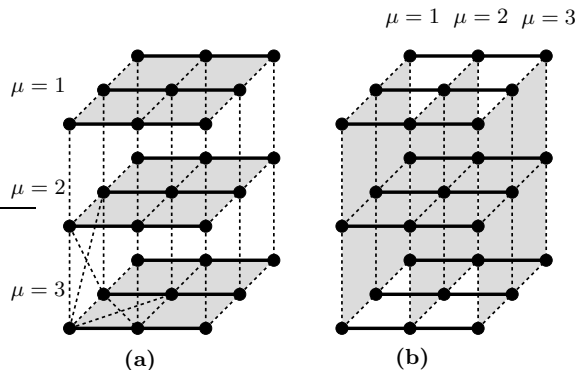
Figure 4.1.: Partition schemes for investigating the transport perpendicular (a) or parallel (b) to the spin chains. Each spin is represented by a dot, solid lines indicate Heisenberg interactions along the chains, dashed lines represent random interactions. The diagonal couplings within each plane have been left out for clarity [except lower left corner of (a)].

4.1. Description of the Model

The model we are going to investigate is a three-dimensional spin model depicted in Fig. 4.1. We perform a partition into N identical subunits (planes), each consisting of n spins. A local magnetic field is present at each spin resulting in a Zeeman splitting of

$$\hat{H}_Z = \frac{\Delta E}{2} \sum_i \hat{\sigma}_z^{(i)}. \tag{4.1}$$

In one direction, the spins are coupled via a Heisenberg interaction

$$\hat{H}_H = \lambda_H \sum_i \hat{\boldsymbol{\sigma}}^{(i)} \otimes \hat{\boldsymbol{\sigma}}^{(i+1)}, \tag{4.2}$$

with the coupling strength λ_H and the Pauli spin vectors $\hat{\boldsymbol{\sigma}}^{(i)} = (\hat{\sigma}_x^{(i)}, \hat{\sigma}_y^{(i)}, \hat{\sigma}_z^{(i)})$. In the other two directions, we use an interaction matrix $\hat{H}_R$ for adjacent spins and next neighbor spins lying diagonally opposite [see lower left corner of Fig. 4.1(a)]. The nonzero matrix elements are taken from a Gaussian ensemble with zero mean and a variance s^2 that is related to the coupling strength λ_R via

$$\lambda_R^2 = \frac{d}{N} s^2, \tag{4.3}$$

with d being the connectivity of the spins. Thus the total Hamiltonian is described by

$$\hat{H} = \hat{H}_Z + \hat{H}_H + \hat{H}_R. \tag{4.4}$$

The coupling strengths λ_H for the Heisenberg interaction and λ_R for the random interaction are chosen so that $\lambda_R \ll \lambda_H \ll \Delta E$. Regardless of the partition scheme chosen
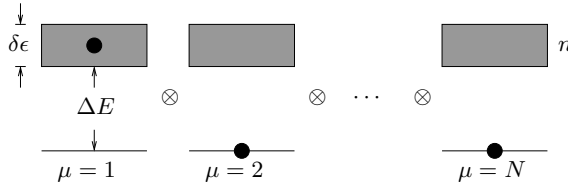
Figure 4.2.: N subunits with ground state and first excitation band of width $\delta\varepsilon$ containing n energy levels each. Black dots specify the initial states used.

each subunit can be seen as a molecule consisting of several energy bands. If we restrict ourselves to initial states where only one spin is excited (or superpositions thereof) the Heisenberg interaction does not allow to leave this subspace of the total Hilbert space. By choosing also the random interaction to conserve the subspace we restrict all further investigations to the single excitation subspace. Therefore, energy transport in our model system is equivalent to spin transport in a gapless system (i.e. $\Delta E = 0$). Figure 4.2 gives a graphical representation of our system, with $\delta\varepsilon$ being the width of the first energy band.

Depending on the partition scheme the heat transport in two alternative directions can be studied: perpendicular to the spin chains [Fig. 4.1(a)] and parallel to them [Fig. 4.1(b)].

4.2. The Time-Convolutionless (TCL) Projection Operator Technique

To investigate transport behavior according to our method it is necessary to partition the total microscopic system described by the Hamiltonian $\hat{H}$ into mesoscopic local subunits. While the complete dynamics is governed by the Schrödinger equation of the full system according to its density operator

$$\dot{\hat{\rho}} = -\mathrm{i}[\hat{H}, \hat{\rho}] \equiv \mathcal{L}(t)\hat{\rho}, \tag{4.5}$$

we aim at deriving a closed reduced dynamical equation for the subunits chosen. This is done by introducing a projection superoperator $\mathcal{P}$ that projects onto the relevant part of the full density matrix $\hat{\rho}$ [Breuer02]. The dynamics of the reduced system is no longer unitary, but described by

$$\mathcal{P}\dot{\hat{\rho}} = \mathcal{P}\mathcal{L}(t)\hat{\rho}. \tag{4.6}$$

Accordingly, we define another projection superoperator $\mathcal{Q}$ projecting on the irrelevant part of the full density matrix $\hat{\rho}$, i.e.,

$$\mathcal{Q}\hat{\rho} = \hat{\rho} - \mathcal{P}\hat{\rho}, \tag{4.7}$$

leading to the dynamics described by

$$\mathcal{Q}\dot{\hat{\rho}} = \mathcal{Q}\mathcal{L}(t)\hat{\rho}. \tag{4.8}$$

4. Heat Transport in Magnetic Systems

In order to be projection operators onto different parts of the system the properties

$$\mathcal{P} + \mathcal{Q} = I \tag{4.9}$$
$$\mathcal{P}^2 = \mathcal{P} \tag{4.10}$$
$$\mathcal{Q}^2 = \mathcal{Q} \tag{4.11}$$
$$\mathcal{P}\mathcal{Q} = \mathcal{Q}\mathcal{P} = 0, \tag{4.12}$$

where I is the identity operation, have to be fulfilled. Using (4.9) in (4.6) and (4.8) leads to the differential equations

$$\mathcal{P}\dot{\hat{\rho}} = \mathcal{P}\mathcal{L}(t)\mathcal{P}\hat{\rho} + \mathcal{P}\mathcal{L}(t)\mathcal{Q}\hat{\rho} \tag{4.13}$$
$$\mathcal{Q}\dot{\hat{\rho}} = \mathcal{Q}\mathcal{L}(t)\mathcal{P}\hat{\rho} + \mathcal{Q}\mathcal{L}(t)\mathcal{Q}\hat{\rho}. \tag{4.14}$$

One possibility to tackle these equations is to formally solve (4.14) for $\mathcal{Q}\hat{\rho}$, resulting in

$$\mathcal{Q}\hat{\rho}(t) = \int_{t_0}^{t} \mathrm{d}s\, \mathcal{G}(t,s)\mathcal{Q}\mathcal{L}(s)\mathcal{P}\hat{\rho}(s), \tag{4.15}$$

with an appropriate propagator $\mathcal{G}(t,s)$. Furthermore, we have assumed factorizing initial conditions, i.e., $\mathcal{Q}\hat{\rho}(t_0) = 0$. Plugging (4.15) into (4.13) leads to an integro-differential equation known as the Nakajima-Zwanzig equation [Nakajima58; Zwanzig60]. Although it allows for a systematic perturbation expansion its structure is usually very complicated because every order requires the integration over superoperators involving the complete history of $\mathcal{P}\hat{\rho}$. Therefore, its applicability to typical physical systems is rather limited [Breuer02].

A different approach tries to explicitly avoid the integral over the complete history by looking at the inverse of the time evolution. We replace the $\hat{\rho}(s)$ in (4.15) by

$$\hat{\rho}(s) = G(t,s)(\mathcal{P} + \mathcal{Q})\hat{\rho}(t), \tag{4.16}$$

where $G(t,s)$ is the backward propagator of the full system, i.e., the inverse of its unitary evolution. We then can write (4.15) as

$$\mathcal{Q}\hat{\rho}(t) = \Sigma(t)(\mathcal{P} + \mathcal{Q})\hat{\rho}(t), \tag{4.17}$$

where we have introduced the superoperator

$$\Sigma(t) = \int_{t_0}^{t} \mathrm{d}s\, \mathcal{G}(t,s)\mathcal{Q}\mathcal{L}(s)\mathcal{P}G(t,s). \tag{4.18}$$

We then move all occurrences of $\mathcal{Q}\hat{\rho}(t)$ in (4.17) to the left-hand side. The superoperator $1 - \Sigma(t)$ may be inverted for small times or small couplings [Breuer02], leading to

$$\mathcal{Q}\hat{\rho}(t) = [1 - \Sigma(t)]^{-1}\mathcal{P}\hat{\rho}(t). \tag{4.19}$$

Plugging this result into (4.13) brings us to a differential equation for the relevant part of the system, i.e.,

$$\mathcal{P}\dot{\hat{\rho}}(t) = \mathcal{P}\mathcal{L}(t)[1 - \Sigma(t)]^{-1}\mathcal{P}\hat{\rho}(t). \tag{4.20}$$

Since this differential equation for the relevant part does not involve a convolution integral like in the Nakajima-Zwanzig equation, this is called the "time-convolutionless" (TCL) master equation [Shibata77]. For convenience, we use in the following the TCL generator

$$\mathcal{K}(t) = \mathcal{P}\mathcal{L}(t)[1 - \Sigma(t)]^{-1}\mathcal{P}. \tag{4.21}$$

In order to perform a perturbation expansion of $\mathcal{K}(t)$ we rewrite $[1 - \Sigma(t)]^{-1}$ as a geometric series, i.e,

$$[1 - \Sigma(t)]^{-1} = \sum_n \Sigma(t)^n, \tag{4.22}$$

we may expand the TCL generator as

$$\mathcal{K}(t) = \sum_n \mathcal{P}\mathcal{L}(t)\Sigma(t)^n\mathcal{P} \equiv \sum_n \lambda^n \mathcal{K}_n(t), \tag{4.23}$$

where λ is the coupling constant in which the series expansion is performed. One may then use (4.18) and the series expansion of $\mathcal{G}(t, s)$ and $G(t, s)$ to compute the $\mathcal{K}_n$. For typical interactions, the odd terms of the series expansion vanish [Breuer02], while the leading order is given by

$$\mathcal{K}_2 = \int_0^t \mathrm{d}t_1 \mathcal{P}\mathcal{L}(t)\mathcal{L}(t_1)\mathcal{P}, \tag{4.24}$$

leading to the second-order TCL master equation

$$\mathcal{P}\dot{\hat{\rho}} = \int_0^t \mathrm{d}t_1 \mathcal{P}\mathcal{L}(t)\mathcal{L}(t_1)\mathcal{P}\hat{\rho}. \tag{4.25}$$

It is important to note that $\mathcal{P}$ has not been specified so far. Apart from the usual requirement for a projection superoperator (4.10) the partition into system of interest and the irrelevant part is largely arbitrary [Breuer07]. However, in order to obtain a converging perturbation series expansion there are constraints to the choice $\mathcal{P}$: A "wrong" partitioning strategy may lead to a breakdown of the expansion [Breuer06].

4.3. Classification of the transport behavior

In order to be able to characterize the transport behavior one needs to introduce a quantity that unambiguously determines whether the transport in a system is ballistic or diffusive. An obvious choice would be the existence of non-vanishing currents in absence of external fields or gradients as a sufficient condition for ballistic transport.

However, this is difficult to implement computationally, as currents in diffusive systems decay exponentially, meaning that even there, small currents will always be present for finite times. A better concept is to look at the spatial variance of an initially peaked excitation

$$\sigma^2(t) = \int \mathrm{d}x \rho(x,t)(x - \bar{x})^2, \tag{4.26}$$

where $\rho(x,t)$ is the probability density and $\bar{x}$ the spatial expectation value.

4.3.1. Variance of a free particle

A free (quasi-)particle not interacting with any external potential shows ballistic transport behavior by definition. We express its Hamiltonian by using the dispersion relation for real particles, i.e.,

$$\hat{H} = \frac{\hat{p}^2}{2m}, \tag{4.27}$$

with $\hat{p}$ being the momentum operator of the particle and m being the mass. In the momentum space the Schrödinger equation reads

$$\mathrm{i}\frac{\partial}{\partial t}\psi(p,t) = \frac{p^2}{2m}\psi(p,t), \tag{4.28}$$

which has the solution

$$\psi(p,t) = \mathrm{e}^{-\mathrm{i}\frac{p^2}{2m}t}\psi(p,0). \tag{4.29}$$

$\psi(p,0)$ is determined by the initial conditions. For a Gaussian wave-packet with initial spatial variance σ_0^2 we obtain for the probability distribution in real space

$$\rho(x,t) = |\psi(x,t)|^2 = \frac{\sqrt{2}\sigma_0}{\sqrt{4\pi\sigma_0^4 + m^2\pi t^2}}\mathrm{e}^{-\frac{2\sigma_0^2 x^2}{4\sigma_0^4 + m^2 t^2}}. \tag{4.30}$$

Its spatial variance (4.26) is given by

$$\sigma^2(t) = \sigma_0^2 + \frac{m^2 t^2}{4\sigma_0^2}. \tag{4.31}$$

This means that ballistic transport implies a variance growing quadratically in time.

4.3.2. Diffusion equation

In contrast to the free particle case we now study the transport behavior of a system whose probability density $\rho(x,t)$ is described by a diffusion equation

$$\frac{\partial\rho}{\partial t} = D\Delta\rho, \tag{4.32}$$

with D being the diffusion coefficient. For an initial probability density

$$\rho(x,0) = \delta(x) \tag{4.33}$$

the solution to (4.32) is

$$\rho(x,t) = \frac{1}{\sqrt{4\pi Dt}} \exp\left(-\frac{x^2}{4Dt}\right). \tag{4.34}$$

This leads to a spatial variance of

$$\sigma^2(t) = 2Dt, \tag{4.35}$$

i.e., for diffusive systems the variance grows linearly. Therefore, the spatial variance is a useful concept for classifying the transport behavior of a system.

However, if we consider instead the differential equation

$$\frac{\partial \rho}{\partial t} = \tilde{D}t\Delta\rho, \tag{4.36}$$

we obtain the solution

$$\rho(x,t) = \frac{1}{\sqrt{2\pi \tilde{D}t^2}} \exp\left(-\frac{x^2}{2Dt^2}\right). \tag{4.37}$$

This results in a spatial variance of

$$\sigma^2(t) = \tilde{D}t^2, \tag{4.38}$$

which means that the transport behavior is ballistic.

4.4. Perpendicular transport

4.4.1. Derivation of the TCL master equation

For the transport perpendicular to the spin chains, the subunit Hamiltonian of our model system is given by

$$\hat{H} = \sum_{\mu=1}^{N} \hat{H}_L(\mu) + \hat{H}_R(\mu, \mu+1), \tag{4.39}$$

where $\hat{H}_L$ consists of a constant local energy splitting, a Heisenberg interaction (i.e. the spin chains) and the internal random couplings of each subunit [cf. gray planes in Fig 4.1(a)]. Since $\lambda_R \ll \lambda_H$ the effect of the internal random couplings on the spectrum of $\hat{H}_L$ may be neglected. The eigenenergies E_i of the first excitation band of an n-spin Heisenberg chain can be computed using the Bethe ansatz [Schollwöck04], leading to

$$E_i = 4\lambda\left(1 + \cos\frac{2\pi i}{n}\right). \tag{4.40}$$

Therefore, the bandwidth $\delta\varepsilon$ is given by

$$\delta\varepsilon = 8\lambda_H. \tag{4.41}$$

$\hat{H}_R(\mu, \mu + 1)$ denotes the interaction between the subunits, which is purely random.

The projection superoperator $\mathcal{P}$ of the type as suggested by Breuer [Breuer07] reads

$$\mathcal{P}\hat{\rho} = \sum_\mu \text{Tr}\left\{\hat{\Pi}_\mu \hat{\rho}\right\} \frac{1}{n}\hat{\Pi}_\mu \equiv \sum_\mu P_\mu \frac{1}{n}\hat{\Pi}_\mu, \tag{4.42}$$

with $\hat{\Pi}_\mu$ being the standard projection operators

$$\hat{\Pi}_\mu = \sum_{n_\mu} |n_\mu\rangle\langle n_\mu|, \tag{4.43}$$

and $|n_\mu\rangle$ the eigenstate of $\hat{H}_L(\mu)$ in the one-particle excitation subspace, i.e. the states in the band of subunit μ (cf. Fig. 4.2). Consequently, the numbers P_μ are just the excitation probabilities of subunit μ.

Switching to the interaction picture, where

$$\hat{V}(t) = \exp(\mathrm{i}\hat{H}_L t)\hat{H}_R \exp(-\mathrm{i}\hat{H}_L t), \tag{4.44}$$

plugging both the Hamiltonian (4.39) and the projection (4.42) into the second-order TCL expansion (4.25), we get

$$\mathcal{P}\frac{\mathrm{d}}{\mathrm{d}t}\hat{\rho} = -\int_0^t \mathrm{d}t_1 \mathcal{P}\left[\hat{V}, \left[\hat{V}(t_1), \mathcal{P}\hat{\rho}\right]\right] = -\sum_\nu \int_0^t \mathrm{d}t_1 \mathcal{P}\left[\hat{V}, \left[\hat{V}(t_1), P_\nu \frac{1}{n}\hat{\Pi}_\nu\right]\right], \tag{4.45}$$

which leads, after performing the projections, to

$$\sum_\sigma \dot{P}_\sigma \frac{1}{n}\hat{\Pi}_\sigma = -\sum_{\mu\nu} \int_0^t \mathrm{d}t_1 \frac{1}{n^2}\text{Tr}\left\{\left[\hat{V}, \left[\hat{V}(t_1), \hat{\Pi}_\nu\right]\right]\right\} P_\nu \hat{\Pi}_\mu. \tag{4.46}$$

Since the projection operators satisfy the relation

$$\hat{\Pi}_\mu \hat{\Pi}_\sigma = \delta_{\mu\sigma}\hat{\Pi}_\mu, \tag{4.47}$$

we only need to look at terms where the first summation indices are equal, arriving at

$$\dot{P}_\mu = -\sum_\nu \int_0^t \mathrm{d}t_1 \frac{1}{n}\text{Tr}\left\{\hat{\Pi}_\mu\left[\hat{V}(t), \left[\hat{V}(t_1), \hat{\Pi}_\nu\right]\right]\right\} P_\nu. \tag{4.48}$$

By inserting the definition of $\hat{V}$ (4.44) and exploiting that $\hat{\Pi}_\mu$ projects onto eigenstates of $\hat{H}_L(\mu)$ we can evaluate the trace by using the block structure of $\hat{H}_R$, resulting in (see [Michel05; Michel06])

$$\dot{P}_\mu = \sum_{k,l}^n 2|\langle k_\mu|\hat{H}_R|l_{\mu+1}\rangle|^2 \frac{\sin\omega_{kl}t}{n\omega_{kl}}\left(P_{\mu+1} - 2P_\mu + P_{\mu-1}\right), \tag{4.49}$$
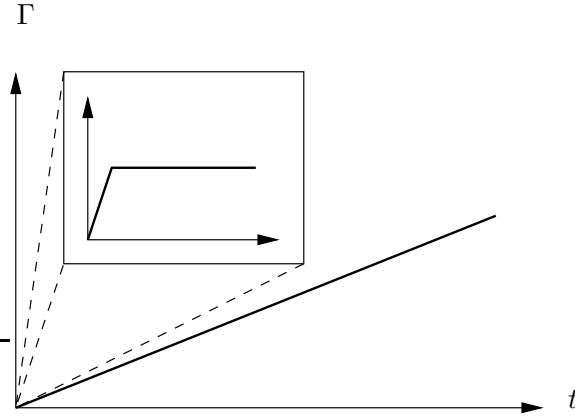
Figure 4.3.: Various regimes for the correlation function Γ. Inset: square and linear regime.

where $\hbar\omega_{kl}$ denotes the energy difference between the eigenstates k, l.

During the time evolution of the system there are three different regimes: For times much smaller than the eigenfrequencies ω_{kl} the double sum

$$\Gamma = \sum_{kl} 2\frac{\sin\omega t}{\omega} \tag{4.50}$$

may be simply replaced by a double sum over the peaks of the sinc functions. This is the so-called "square regime", resulting in

$$\Gamma = 2n^2 t. \tag{4.51}$$

The term "square regime" comes from the transition probabilities growing quadratically in time. The correlation function Γ, however, grows linearly in this case.

After some time, however, the difference in the eigenfrequencies becomes observable. This is the linear regime, which may be computed analogously to Fermi's Golden Rule (see below).

For very large times, the argument of the sine function is merely a random phase, which makes its contribution vanish after summation. Therefore, in this regime only terms with $k = l$ contribute, leading to

$$\Gamma = 2nt. \tag{4.52}$$

While in this regime Γ grows linearly in time as in the square regime, the slope is smaller by a factor of n. Figure 4.3 shows typical behavior of Γ over time.

Assuming $|\langle k_\mu|\hat{H}_R|l_{\mu+1}\rangle|^2 \approx \lambda_R^2$, the double sum can be computed analogous to Fermi's Golden Rule [Schwabl98]. We consider the distribution

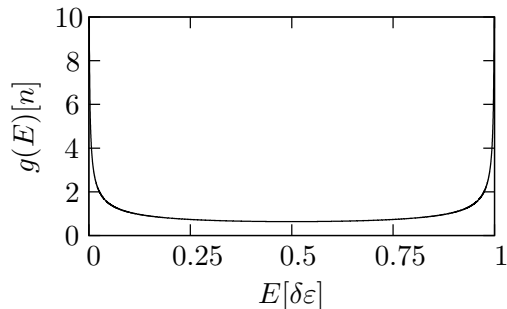$$\delta_t(\omega) = \frac{\sin\omega t}{\pi\omega}, \tag{4.53}$$

Figure 4.4.: Density of states for the first excitation band of a Heisenberg chain.

which is a representation of the Dirac δ-distribution, i.e.,

$$\lim_{t \to \infty} \int_{-\infty}^{\infty} F(\omega)\delta_t(\omega)\mathrm{d}\omega = F(0). \tag{4.54}$$

Therefore, we may write for the relaxation rate

$$\gamma = 2\lambda^2 \sum_{k,l} \frac{\sin \omega_{kl} t}{n \omega_{kl}} = \frac{2\pi\lambda^2}{n} \sum_{k,l} \delta(E_k - E_l). \tag{4.55}$$

Replacing the double sum over integrals in the energy space we arrive at

$$\gamma = \frac{2\pi\lambda^2}{n} \int_0^{\delta\varepsilon} g(E)^2 \mathrm{d}E, \tag{4.56}$$

i.e., the integral over the square of the density of states. Using (4.40), the density of states of the first excitation band of a Heisenberg chain is given by

$$
\begin{aligned}
g(E) &= \sum_i \delta(E - E_n) \approx \frac{n}{\pi} \int_0^{\pi} \mathrm{d}x \, \delta\left[E - \frac{\delta\varepsilon}{2}(1 + \cos x)\right] \\
&= \frac{2n}{\pi\delta\varepsilon} \int_0^1 \mathrm{d}u \frac{1}{\sqrt{1 - u^2}} \delta\left[u - \left(\frac{2E}{\delta\varepsilon}\right)\right] = \frac{2n}{\pi\delta\varepsilon} \frac{1}{\sqrt{1 - \left(\frac{2E}{\delta\varepsilon} - 1\right)^2}}.
\end{aligned} \tag{4.57}
$$

Figure 4.4 shows a plot of $g(E)$.

Unfortunately, (4.57) is not square integrable due to the singularities at the boundaries of the spectrum. In order to obtain a finite result, we renormalize the number of states in the band. Renormalization is a procedure originally developed in quantum field theory [Bjorken65], but can be regarded as a mathematical tool as well [Delamotte04].

We introduce the regularized integral

$$F_\Lambda(n) = \int_\Lambda^{\delta\varepsilon} \frac{\alpha^2 n^2}{\pi^2 E(\delta\varepsilon - E)}, \tag{4.58}$$

with α being the factor the renormalizes the number of states. We assume that for a band consisting of only a few levels $\tilde{n}$ (but still enough to define a density of states), the density of states is approximately constant. Our renormalization prescription is then given by

$$F_\Lambda(\tilde{n}) = \frac{\tilde{n}^2}{\delta\varepsilon}, \tag{4.59}$$

resulting in

$$\alpha = \frac{\pi}{\sqrt{2\log(\delta\varepsilon/\Lambda - 1)}}. \tag{4.60}$$

This allows us to calculate the physical limit of the renormalization procedure, i.e.,

$$\lim_{\Lambda \to 0} F_\Lambda(n) = \frac{n^2}{\delta\varepsilon}, \tag{4.61}$$

which is the same value as for a constant density of states. This finally leads to the rate equations

$$\frac{\mathrm{d}P_1}{\mathrm{d}t} = \gamma(P_2 - P_1) \tag{4.62}$$

$$\frac{\mathrm{d}P_\mu}{\mathrm{d}t} = \gamma(P_{\mu+1} - 2P_\mu + P_{\mu-1}) \tag{4.63}$$

$$\frac{\mathrm{d}P_N}{\mathrm{d}t} = \gamma(P_{N-1} - P_N) \tag{4.64}$$

with the relaxation rate

$$\gamma = \frac{2\pi\lambda_R^2 n}{\delta\varepsilon}. \tag{4.65}$$

The approximation introduced by Fermi's Golden Rule is only valid in the linear regime, i.e.

$$\frac{4\pi^2 n\lambda_R^2}{\delta\varepsilon^2} \ll 1. \tag{4.66}$$

4.4.2. Solution of the TCL master equation

For a system consisting of 3 subunits (4.62–4.64) can be solved easily, resulting in

$$\begin{aligned}
P_1(t) &= \frac{1}{6}(2 + \mathrm{e}^{-3\gamma t} + 3\mathrm{e}^{-\gamma t}) \\
P_1(t) &= \frac{1}{3}(1 - \mathrm{e}^{-3\gamma t}) \\
P_1(t) &= \frac{1}{6}(2 + \mathrm{e}^{-3\gamma t} - 3\mathrm{e}^{-\gamma t}).
\end{aligned} \tag{4.67}$$

Figure 4.5 shows both the numerical results for the solution of the full Schrödinger equation and the solution of the rate equation (4.63), which are in reasonably good agreement.

Equation (4.63) is a discrete version of the diffusion equation. For a δ-shaped excitation at $t = 0$ its solution is a Gaussian function whose variance grows linear in time.
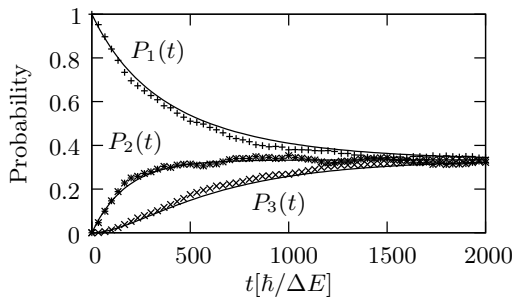
Figure 4.5.: Perpendicular transport: probability to find the excitation in subunit $\mu = 1, 2, 3$. Comparison of the numerical solution of the Schrödinger equation (crosses) and second-order TCL (lines). ($N = 3$, $n = 600$, $\lambda_R = 5 \cdot 10^{-4}$, $\lambda_H = 6.25 \cdot 10^{-2}$)

Therefore, it is evident that the heat transport is normal perpendicular to the chains. Furtheremore, in our model diffusive behavior is an emergent property, as the dynamics of a single spin is obviously non-diffusive.

4.4.3. Thermal conductivity

The thermal conductivity can be calculated by considering states close to equilibrium. In this case, we still have a temperature difference ΔT between adjacent subunits. Then, the thermal conductivity is given by

$$\kappa = \gamma n \left(\frac{\Delta E}{T} \right)^2 \frac{\mathrm{e}^{-\Delta E/T}}{\left(1 + n\mathrm{e}^{-\Delta E/T}\right)^2}, \tag{4.68}$$

with T being the mean temperature between adjacent subunits [Michel05].

4.4.4. Lower-dimensional systems

One might be tempted to ask whether this transport behavior can be observed in lower-dimensional systems as well. The crucial parameter is the connectivity d between adjacent planes. For our three-dimensional model we have $d = 9$, which reduces to $d = 3$ in a 2D system. In order to study the deviation from normal transport behavior, we consider the time-averaged quadratic deviation

$$D_1^2 = \frac{1}{\tau} \int_0^\tau [P_1^{\mathrm{TCL}}(t) - P_1^{\mathrm{S}}(t)]^2 \mathrm{d}t, \tag{4.69}$$

with $P_1^{\mathrm{TCL}}(t)$ being the solution of the TCL master equation (4.67) and $P_1^{\mathrm{S}}(t)$ being the numerical solution of the time-dependent Schrödinger equation. Figure 4.6 shows the deviation for different connectivities. Connectivities larger than for the 3D case have been obtained by including more couplings between adjacent plains. These results are
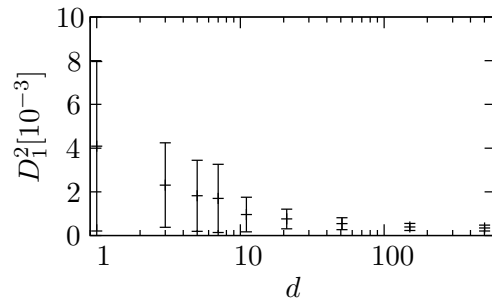
Figure 4.6.: Deviation from normal transport over connectivity. ($N = 3$, $n = 500$, $\lambda_R = 5 \cdot 10^{-4}$, $\lambda_H = 6.25 \cdot 10^{-2}$, average and standard deviation for 75 random interaction matrices)

largely independent of the size of the subunits. Therefore, in 2D systems the deviation from normal transport will always be significantly larger than in a 3D system.

4.5. Parallel transport

4.5.1. General properties of the interactions

In the following let us concentrate on the other direction, i.e., parallel to the chains. Thus, we have a slightly different partition of the total Hamiltonian,

$$\hat{H} = \sum_{\mu=1}^{N} \hat{H}_L^{(\mu)} + \hat{H}_H^{(\mu,\mu+1)} + \hat{H}_R^{(\mu,\mu+1)} \equiv \hat{H}_L + \hat{H}_H + \hat{H}_R. \tag{4.70}$$

Here, the local part $\hat{H}_L$ contains only random interactions besides the Zeeman splitting. In the one-particle excitation space the Hamiltonian for the Heisenberg interaction can be written as

$$\hat{H}_H = 2\lambda_H \begin{pmatrix} & \hat{1} & \\ \hat{1} & & \hat{1} \\ & \hat{1} & \ddots \end{pmatrix}. \tag{4.71}$$

The local Hamiltonian $\hat{H}_L$ has features a diagonal block structure

$$\hat{H}_L = \begin{pmatrix} \hat{H}_L^{(\mu)} & & \\ & \hat{H}_L^{(\mu+1)} & \\ & & \ddots \end{pmatrix}. \tag{4.72}$$

35

Therefore, the commutator $[\hat{H}_H, \hat{H}_L]$ is given by

$$[\hat{H}_H, \hat{H}_L] = 2\lambda_H \begin{pmatrix} & \hat{H}_L^{(\mu+1)} - \hat{H}_L^{(\mu)} & \\ \hat{H}_L^{(\mu)} - \hat{H}_L^{(\mu+1)} & & \hat{H}_L^{(\mu+2)} - \hat{H}_L^{(\mu+1)} \\ & \hat{H}_L^{(\mu+1)} - \hat{H}_L^{(\mu+2)} & \ddots \end{pmatrix}. \quad (4.73)$$

Since all operators $\hat{H}_L^{(\mu)}$ have matrix elements drawn from the same ensemble, the commutator will vanish for sufficiently large matrix sizes.

The Hamiltonian for the random interaction between the subunits has a block structure similar to $\hat{H}_H$, i.e.,

$$\hat{H}_R = \begin{pmatrix} & \hat{H}_R^{(\mu,\mu+1)} & \\ \hat{H}_R^{(\mu,\mu+1)\dagger} & & \hat{H}_R^{(\mu+1,\mu+2)} \\ & \hat{H}_R^{(\mu+1,\mu+2)\dagger} & \ddots \end{pmatrix}. \quad (4.74)$$

Using the same argument as above the commutator $[\hat{H}_H, \hat{H}_R]$ vanishes as well. In summary, the commutator relations

$$[\hat{H}_H, \hat{H}_L] = [\hat{H}_H, \hat{H}_R] = 0 \quad (4.75)$$

are satisfied. If the dynamics induced by $\hat{H}_L$ and $\hat{H}_H$ is absorbed in the transformation into the interaction picture, the random interaction transforms into

$$\hat{V}(t) = e^{i(\hat{H}_H + \hat{H}_L)t} \hat{H}_R e^{-i(\hat{H}_H + \hat{H}_L)t} = e^{i\hat{H}_L t} \hat{H}_R e^{-i\hat{H}_L t}, \quad (4.76)$$

where (4.75) has been used. Therefore, the derivation of the dynamics of the P_μ (4.49) is still valid.

4.5.2. Local band structure

For calculating the local band structure we consider a random matrix of dimension n, drawn from a Gaussian unitary ensemble. For such a matrix the density of states is given by (see [Mehta91])

$$g(E) = \frac{8n}{\pi \delta\varepsilon} \sqrt{\frac{\delta\varepsilon^2}{4} - E^2}. \quad (4.77)$$

Using (4.3), the width of the energy band is

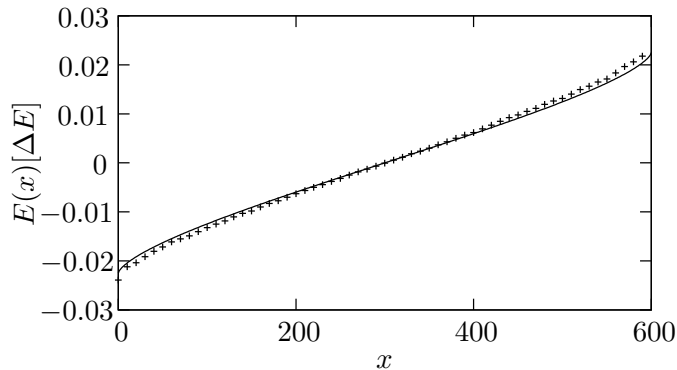$$\delta\varepsilon = 4\frac{n^2 \lambda_R^2}{d}. \quad (4.78)$$

Figure 4.7.: Comparison of the eigenvalues of $\hat{H}_L$ and a random matrix drawn from a Gaussian unitary ensemble. ($n = 600$, $\lambda_R = 5 \cdot 10^{-4}$, $d = 8$)

In order to check whether our local Hamiltonian $\hat{H}_L$ can be approximated by such a random matrix, we compare the eigenvalues $E(x)$. For the random matrix we use

$$n = \int_0^n \mathrm{d}x = \int_{-\delta\epsilon/2}^{\delta\epsilon/2} g(E)\mathrm{d}E \qquad (4.79)$$

leading to

$$\frac{\mathrm{d}E}{\mathrm{d}x} = \frac{1}{g[E(x)]}. \qquad (4.80)$$

Separation of variables yields

$$\frac{8n}{\pi\delta\varepsilon}\sqrt{\frac{\delta\varepsilon^2}{4} - E^2}\,\mathrm{d}E = \mathrm{d}x. \qquad (4.81)$$

This expression cannot be solved analytically for E, so we compare the numerical solution for discrete values of x with the actual eigenvalues of $\hat{H}_L$. As Fig.4.7 shows, $\hat{H}_L$ may indeed be approximated by a random matrix drawn from a Gaussian unitary ensemble. However, by looking at (4.78) and (4.66) that the requirement for the linear regime is violated and the derivation according to Fermi's Golden Rule can no longer be applied.

4.5.3. Solution of the TCL master equation

Instead of using Fermi's Golden Rule argument we approximate the sinc function in (4.49) by its peak value and obtain for the diffusion coefficient

$$\gamma = 2n\lambda_R^2 t, \qquad (4.82)$$

which is linear in time.

37

4. Heat Transport in Magnetic Systems

The solution of (4.63) with the diffusion coefficient (4.82) defines the occupation probabilities in the interaction picture P_μ^{int}. Since we are interested in the occupation probabilities in the Schrödinger picture P_μ^{s} we need to calculate the inverse transformation of the density operator

$$\mathcal{P}\hat{\rho}^{\text{s}} = e^{-i\hat{H}_H t}\mathcal{P}\hat{\rho}^{\text{int}}e^{i\hat{H}_H t}, \tag{4.83}$$

where the diagonal elements $\mathcal{P}\hat{\rho}^{\text{s}}_{\mu\mu}$ are the occupation probabilities P_μ^{s}. The off-diagonal elements of $\mathcal{P}\hat{\rho}^{\text{int}}$ can be computed by replacing the projector (4.43) with another one projecting out off-diagonal elements as well, i.e,

$$\mathcal{P}\hat{\rho} = \sum_\mu \text{Tr}\left\{\hat{\Pi}_{\mu\nu}\hat{\rho}\right\}\frac{1}{n}\hat{\Pi}_{\mu\nu} \equiv \sum_{\mu\nu}\hat{\rho}^{\text{int}}_{\mu\nu}\frac{1}{n}\hat{\Pi}_{\mu\nu}, \tag{4.84}$$

with

$$\hat{\Pi}_{\mu\nu} = \sum_n |n_\mu\rangle\langle n_\nu|. \tag{4.85}$$

The master equation for the off-diagonal elements is always of the form

$$\frac{\text{d}}{\text{d}t}\hat{\rho}^{\text{int}}_{\mu\nu} = -\kappa_{\mu\nu}\hat{\rho}^{\text{int}}_{\mu\nu}, \tag{4.86}$$

with a positive relaxation coefficient κ. This means that the dynamics of the diagonal and the off-diagonal elements decouple so that diagonal initial states remain diagonal for all time.

Solving the TCL master equation first in the interaction picture for 3 subunits gives

$$\begin{aligned}
P_1^{\text{int}}(t) &= \frac{1}{6}\left(2 + e^{-3\lambda_R^2 n t^2} + 3e^{-\lambda_R^2 n t^2}\right) \\
P_2^{\text{int}}(t) &= \frac{1}{3}\left(1 - e^{-3\lambda_R^2 n t^2}\right) \\
P_3^{\text{int}}(t) &= \frac{1}{6}\left(2 + e^{-3\lambda_R^2 n t^2} - 3e^{-\lambda_R^2 n t^2}\right).
\end{aligned} \tag{4.87}$$

Using (4.83) to transform into the Schrödinger picture finally leads to

$$\begin{aligned}
P_1^{\text{s}}(t) &= \frac{1}{24}e^{-3\lambda_R^2 n t^2}\left[12e^{2\lambda_R^2 n t^2}\cos\left(\sqrt{2}\lambda_H t\right) + 8e^{3\lambda_R^2 n t^2} + 3\cos\left(2\sqrt{2}\lambda_H t\right) + 1\right] \\
P_2^{\text{s}}(t) &= \frac{1}{12}e^{-3\lambda_R^2 n t^2}\left[-3\cos\left(2\sqrt{2}\lambda_H t\right) + 4e^{3\lambda_R^2 n t^2} - 1\right] \\
P_3^{\text{s}}(t) &= \frac{1}{24}e^{-3\lambda_R^2 n t^2}\left[-12e^{2\lambda_R^2 n t^2}\cos\left(\sqrt{2}\lambda_H t\right) + 8e^{3\lambda_R^2 n t^2} + 3\cos\left(2\sqrt{2}\lambda_H t\right) + 1\right].
\end{aligned} \tag{4.88}$$

In Fig. 4.8 the numerical solution of the Schrödinger equation is compared with the TCL prediction. Again, there is good agreement between the two methods.
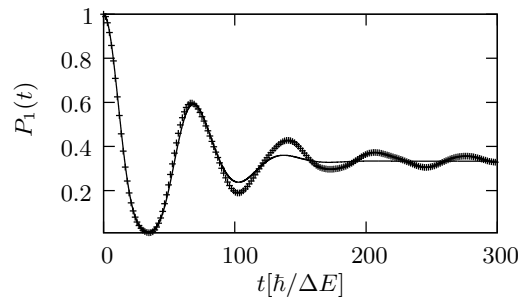
Figure 4.8.: Parallel transport: probability to find the excitation in the first subunit ($\mu = 1$). Comparison of the numerical solution of the Schrödinger equation (crosses) and second-order TCL (solid line). (Same parameters as for Fig. 4.5)
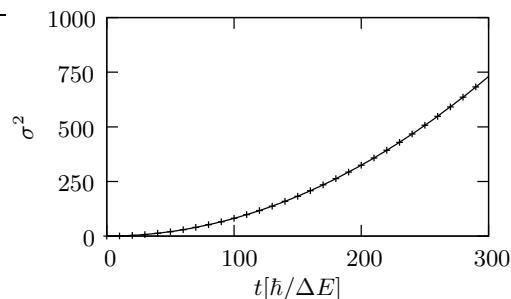

Figure 4.9.: Variance of an excitation initially at subunit $\mu_0 = 150$. Second-order TCL prediction (crosses) and quadratic fit (solid line). ($N = 300$, $n = 600$, $\lambda_R = 5 \cdot 10^{-4}$, $\lambda_H = 6.25 \cdot 10^{-2}$)

4.5.4. Spatial variance

To investigate the transport behavior a much larger system has to be considered, so that the initial excitation does not reach the boundaries of the system during the relaxation time. Since the solution of the time-dependent Schrödinger equation becomes unfeasible, the second-order TCL prediction has been used for subsequent numerical integration. The variance of an excitation initially at $\mu = \mu_0$ shown in Fig. 4.9 grows quadratic in time, i.e. the transport is ballistic. Here we have considered a system with $N = 300$ subunits and an initial excitation at $\mu_0 = 150$ solving the TCL master equation. Numerical investigations show that the transport behavior is largely independent of $\gamma(t)$. Ballistic transport is observed as long as $\lambda_H t \gg \gamma(t)$ on all relevant timescales.

4.6. Discussion

In summary, we have shown that transport properties in a quantum system can be studied from first principles using a projection operator method that projects out the

information on the local sub-structure. We have verified the accuracy of the second-order TCL expansion by comparison with the numerical solution of the full time-dependent Schrödinger equation.

Using this extended projection operator technique [Breuer06; Breuer07] we have analyzed the transport behavior of a concrete spin model system. In agreement with experimental investigations of magnetic systems [Sologubenko00; Hess01] we have found a dramatic anisotropy in the heat conducting behavior of the system: normal behavior perpendicular to strongly coupled Heisenberg spin chains and a ballistic one in the direction of the chains. The results of this analysis supports previous results concerning the transport in spin systems [Heidrich-Meisner03].

In this way diffusive behavior has been derived from first principles on a mesoscopic scale whereas the dynamics on the microscopic scale (i.e. of a single spin) is obviously non-diffusive. This indicates that the transport behavior is not only a property of a system per se, but also depends on the way we are looking at it.

5. Entropy Transport in the Jaynes-Cummings Model

5.1. Jaynes-Cummings model

The Jaynes-Cummings model [Jaynes63] (JCM) is a simple but powerful model describing the interaction between a two-level atom and a single mode of the quantized radiation field. While being exactly solvable it offers a large range of genuinely quantum phenomena like collapses and revivals in the inversion of the atom [Yoo85; Shore93], which have been observed experimentally as well [Rempe87; Brune96]. In the framework of the JCM we will propose a novel procedure for transporting entropy within the atom-field system, allowing to control the temperature of the atom.

5.1.1. Field quantization

Our starting point for the quantization of the radiation field are the Maxwell equations of classical electrodynamics. In free space, without currents and charges they are given by (in Heaviside-Lorentz units, with the speed of light $c = 1$)

$$\nabla \cdot \mathbf{E} = 0 \tag{5.1}$$

$$\nabla \cdot \mathbf{B} = 0 \tag{5.2}$$

$$\nabla \times \mathbf{E} + \frac{\partial}{\partial t}\mathbf{B} = 0 \tag{5.3}$$

$$\nabla \times \mathbf{B} - \frac{\partial}{\partial t}\mathbf{E} = 0. \tag{5.4}$$

Introducing a vector potential $\mathbf{A}$ satisfying

$$\mathbf{B} = \nabla \times \mathbf{A}, \tag{5.5}$$

allows to transform (5.3) and (5.4) to

$$\nabla \cdot (\nabla \cdot \mathbf{A}) - \nabla^2 \mathbf{A} + \frac{\partial^2}{\partial t^2}\mathbf{A} = 0. \tag{5.6}$$

The vector potential is not unambiguously defined as the physical fields $\mathbf{E}$ and $\mathbf{B}$ invariant under the gauge transformation

$$\mathbf{A} \mapsto \mathbf{A}' = \mathbf{A} - \nabla\chi. \tag{5.7}$$

5. Entropy Transport in the Jaynes-Cummings Model

We now introduce a fixed gauge by

$$\nabla \cdot \mathbf{A} = 0, \tag{5.8}$$

which is called the Coulomb gauge. This leads to the wave equation

$$\nabla^2 \mathbf{A} - \frac{\partial^2}{\partial t^2}\mathbf{A} = 0. \tag{5.9}$$

We now regard a volume of periodicity V of arbitrary size, where we may use a mode ansatz for $\mathbf{A}$, i.e.,

$$\mathbf{A} = \sum_k \left(\mathbf{A_k} \exp(\mathrm{i}\mathbf{k}\mathbf{r}) + c.c \right). \tag{5.10}$$

Here $\mathbf{k}$ denotes the wave vector and $\mathbf{r}$ the position. Plugging (5.10) into (5.9) gives

$$\omega^2 \mathbf{A_k} - \frac{\partial^2}{\partial t^2}\mathbf{A_k} = 0, \tag{5.11}$$

which has the solution

$$\mathbf{A_k} = \mathbf{A_k}(0) \, \exp(-\mathrm{i}\omega t). \tag{5.12}$$

Since the solution must respect the Coulomb gauge we obtain solutions for two orthonormal polarization vectors $\mathbf{e}_{k\lambda}$, i.e.,

$$\mathbf{A} = \sum_{k\lambda} \sqrt{\frac{1}{2\omega V}} \, \mathbf{e}_{k\lambda} \left(a_{k\lambda} \, e^{i(\mathbf{k}\mathbf{r}-\omega t)} + a_{k\lambda}^* \, e^{-i(\mathbf{k}\mathbf{r}-\omega t)} \right). \tag{5.13}$$

The time-averaged energy per cycle for a mode k may then be written as

$$\mathcal{E}_k = \frac{\omega}{4\pi} \int_V \mathrm{d}^3 r \int_0^{\frac{2\pi}{\omega}} \mathrm{d}t \left(\mathbf{E_k}^2(\mathbf{r},t) + \mathbf{B_k}^2(\mathbf{r},t) \right) = \frac{1}{2}\omega \left(a^* a + a a^* \right), \tag{5.14}$$

which is formally equivalent to the energy of a quantized harmonic oscillator (2.25). Therefore we use the quantization procedure

$$\begin{aligned} a_{k\lambda} &\mapsto \hat{a}_{k\lambda} \\ a_{k\lambda}^* &\mapsto \hat{a}_{k\lambda}^\dagger. \end{aligned} \tag{5.15}$$

For the derivation of the Hamiltonian of the radiation field we start from the classical Hamilton density

$$\mathcal{H} = \frac{1}{2}\dot{A}_j \dot{A}_j + \frac{1}{2}\frac{\partial A_j}{\partial x_i}\frac{\partial A_j}{\partial x_i}, \tag{5.16}$$

where Einstein summation convention has been used. The Hamiltonian is then given by

$$\hat{H} = \int d^3 r \left(\frac{1}{2}\dot{\hat{A}}_j \dot{\hat{A}}_j + \frac{1}{2}\frac{\partial \hat{A}_j}{\partial x_i}\frac{\partial \hat{A}_j}{\partial x_i} \right), \tag{5.17}$$

with the $\hat{A}_i$ being obtained via the quantization procedure. By using

$$\int d^3r\,\mathbf{u}_{k\lambda}\mathbf{u}^*_{k'\lambda'} = \frac{\hbar}{2\omega}\delta_{kk'}\delta_{\lambda\lambda'} \tag{5.18}$$

we finally obtain for the Hamiltonian

$$\hat{H} = \sum_{k\lambda}\omega_k\left(\hat{a}^\dagger_{k\lambda}\hat{a}_{k\lambda} + \frac{1}{2}\right). \tag{5.19}$$

This means that the quantized radiation field is described by a set of independent harmonic oscillators.

5.1.2. Resonant Interaction Hamiltonian

The Hamiltonian describing atom and field is given by

$$\hat{H} = \int \hat{\Psi}^\dagger\left[\frac{1}{2m}(\hat{\mathbf{p}} - e\hat{\mathbf{A}})^2 + e\phi\right]\hat{\Psi} + \hat{H}_F, \tag{5.20}$$

where e is the electron charge, ϕ is the Coulomb potential and $\hat{H}_F$ is the Hamiltonian of the radiation field (5.19) [Walls94]. $\hat{\Psi}$ is the operator for the Schrödinger field of the atom in second quantization. The term proportional to $\mathbf{A}^2$ is negligible, and if the wavelength of the radiation field is small compared to the linear dimension of the atom we may perform the electric dipole approximation

$$\hat{\mathbf{p}}\hat{\mathbf{A}} \approx -\hat{\mathbf{d}}\hat{\mathbf{E}}, \tag{5.21}$$

where $\mathbf{d}$ is the electric dipole moment. Putting all the pieces together, we finally arrive at

$$\hat{H} = \frac{\Delta E}{2}\hat{\sigma}_z + \omega(\hat{a}^\dagger\hat{a} + \frac{1}{2}) + g(\hat{\sigma}_+\hat{a} + \hat{\sigma}_-\hat{a}^\dagger + \hat{\sigma}_+\hat{a}^\dagger + \hat{\sigma}_-\hat{a}) \tag{5.22}$$

with

$$g = d\sqrt{\frac{\omega}{2V}}. \tag{5.23}$$

For a two-level atom we have

$$\hat{d} = \int \psi^*_e e\hat{x}\psi_g. \tag{5.24}$$

The interaction Hamiltonian is simply given by the last summand in (5.22), i.e.,

$$\hat{H}_I = g(\hat{\sigma}_+\hat{a} + \hat{\sigma}_-\hat{a}^\dagger + \hat{\sigma}_+\hat{a}^\dagger + \hat{\sigma}_-\hat{a}). \tag{5.25}$$

The last two terms lead to oscillations at twice the resonance frequency and may be neglected [Walls94]. This approximation is often called the "rotating wave approximation" (RWA).
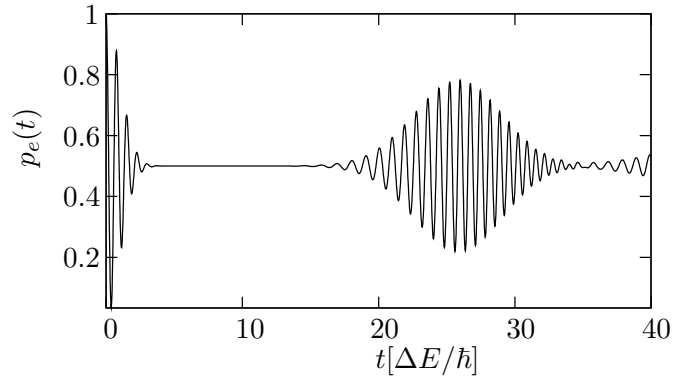
43

Figure 5.1.: Collapse and revival of the probability to find the atom in its excited state $(g = 1, \alpha = 4)$

After performing the RWA the total Hamiltonian can be written as a sum of two-dimensional operators acting only on the states $|e, n\rangle, |g, n + 1\rangle$. In this basis we have

$$\hat{H}_n = \Omega_{n+1}\hat{\sigma}_x, \tag{5.26}$$

with Ω_{n+1} being the Rabi frequency defined by

$$\Omega_n = g\sqrt{n}. \tag{5.27}$$

The eigenstates of (5.26) are well-known and read

$$
\begin{aligned}
|+_n\rangle &= \frac{1}{\sqrt{2}}(|g, n + 1\rangle + |e, n\rangle) \\
|-_n\rangle &= \frac{1}{\sqrt{2}}(|g, n + 1\rangle - |e, n\rangle).
\end{aligned} \tag{5.28}
$$

If the field is initially prepared in a Fock state $|n\rangle$ and the atom in its excited state $|e\rangle$, we obtain Rabi oscillations in the atom as its probability of being in the excited state is given by

$$p_e(t) = |\langle e, n|\hat{U}|e, n\rangle|^2 = \cos^2(\Omega_n t). \tag{5.29}$$

In contrast, if the field starts in a coherent state $|\alpha\rangle$ the evolution of the system is much more complicated and shows collapses and revivals of $p_e(t)$ as shown in Fig. 5.1. The revival can be made perfect when applying a π pulse in the $\hat{\sigma}_z$ basis of the system at half of the revival time. This leads to a complete inversion of the time-evolution of the dynamics and finally to an echo phenomenon as shown in Fig. 5.2.

For a field prepared in a coherent state, the state of the atom will be almost pure at half of the revival time if the atom is initially in a pure state [Gea-Banacloche90; Phoenix91]. However, a more realistic model would involve a thermal initial state for the atom. The thermal contribution to the initial state of the field may be neglected as long as the number of coherent photons is sufficiently larger than the number of thermal photons
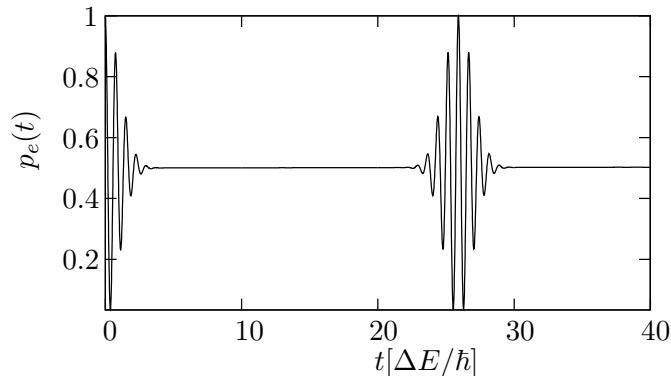
Figure 5.2.: Perfect revival after an additional π pulse. ($g = 1$, $\alpha = 4$)

[Satyanarayana92]. Using thermal states allows for an investigation of the thermal properties of the JCM, i.e., its applicability for problems like the initial state preparation in quantum computing [DiVincenzo00], cooling of atoms [Chu98; Cohen-Tannoudji98; Phillips98], or implementation of quantum thermodynamic machines [Gemmer04].

5.2. Proposed procedure

In the following we will discuss a model where an atom in a thermal state enters a cavity prepared in a coherent state. By obtaining a closed form for the reduced density matrix for the atom we will show that after the collapse the state of the atom is independent of its initial state. After a fixed interaction time the atom is taken to leave the cavity and to interact with a laser field, which is treated as a semi-classical driver. For an appropriate laser field the final state will be thermal as well. Depending on the interaction time with the cavity, the final temperature can be varied over a large range, leading to cooling or heating of the atom. We will present an expression for the minimum and maximum temperature that can be achieved. Finally, we will discuss applications of the method to cooling of the internal degrees of freedom of atoms and creating heat baths suitable for studying thermodynamics at the nanoscale. The whole procedure of our proposal is depicted in Fig. 5.3.

The total system is described by the Hamiltonian

$$\hat{H} = \hat{H}_A + \hat{H}_F + \hat{H}_I, \tag{5.30}$$

where the atomic Hamiltonian $\hat{H}_A$ is given by

$$\hat{H}_A = \frac{\Delta E}{2}\hat{\sigma}_z, \tag{5.31}$$

with ΔE being the energy splitting. The field Hamiltonian $\hat{H}_F$ is

$$\hat{H}_F = \hbar\omega \left(\hat{a}^\dagger \hat{a} + \frac{1}{2} \right), \tag{5.32}$$
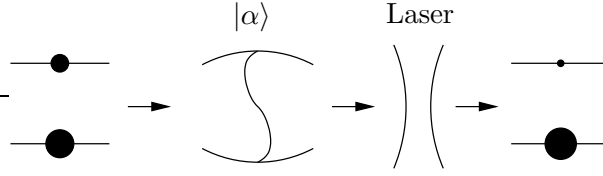
Figure 5.3.: Outline of the procedure: a two-level atom in a thermal state (occupation probabilities represented by black dots) interacts with a cavity prepared in a coherent state $|\alpha\rangle$. After a time t the atom leaves the cavity. A laser pulse is applied to the system, resulting in a thermal state with a different temperature.

with ω being the frequency of the single mode and $\hat{a}$ being the annihilation operator of field mode. Being in resonance, we have $\omega = \Delta E$. The JCM interaction Hamiltonian is given by

$$\hat{H}_I = g\hat{\sigma}^+\hat{a} + g^*\hat{\sigma}^-\hat{a}^\dagger. \tag{5.33}$$

We restrict ourselves to the field being initially in a coherent state $|\alpha\rangle$ and the atom being in a thermal state described by the density operator

$$\hat{\rho}(0) = Z^{-1}\exp(-\beta\hat{H}_A) \equiv p_e(0)|e\rangle\langle e| + [1 - p_e(0)]|g\rangle\langle g|, \tag{5.34}$$

with Z being the partition function, β the inverse temperature, p_e the probability to find the atom in its excited state $|e\rangle$, and $|g\rangle$ denotes its ground state.

5.3. Reduced density matrix for the atom

The time evolution of the full system is then given by

$$\begin{aligned}
\hat{\rho}(t) &= p_e(0)\hat{U}|e,\alpha\rangle\langle e,\alpha|\hat{U}^\dagger + [1 - p_e(0)]\hat{U}|g,\alpha\rangle\langle g,\alpha|\hat{U}^\dagger \\
&\equiv p_e(0)|\psi_e(t)\rangle\langle\psi_e(t)| + [1 - p_e(0)]|\psi_g(t)\rangle\langle\psi_g(t)|,
\end{aligned} \tag{5.35}$$

where $\hat{U}$ is the time evolution operator of the full system.

In order to obtain the effective time evolution for the atom alone, the degrees of freedom corresponding to the field have to be traced out according to (2.17). Here, the partial trace over the field is given by

$$\hat{\rho}(t) = \text{Tr}_F\left\{|\psi(t)\rangle\langle\psi(t)|\right\} = \sum_n \langle n|\psi(t)\rangle\langle\psi(t)|n\rangle. \tag{5.36}$$

Since $\hat{\rho}$ is hermitian and has unit trace, the atom is effectively described by the diagonal element ρ_{11} and the off-diagonal element ρ_{01}.

In the following we first consider the case where the initial state is $|e, \alpha\rangle$. Then, the full time evolution is given by (see, e.g., [Basdevant00])

$$|\psi_e(t)\rangle = \sum_n \left(e^{-i\Omega_{n+1}t/2}|+_{n+1}\rangle - e^{i\Omega_{n+1}t/2}|-_{n+1}\rangle \right) \frac{e^{-|\alpha|^2/2}}{\sqrt{2}} \frac{\alpha^n}{\sqrt{n!}} e^{-i(n+1/2)\omega t}, \qquad (5.37)$$

where the n-photon Rabi frequency Ω_n and the n-photon eigenstates of the atom-field system have been used. The time evolution of the reduced density matrix element ρ_{11} before the revival time has been studied extensively (see, e.g., [Basdevant00]) and is given by

$$\rho_{11}(t) = \frac{1}{2} + \frac{1}{2}\cos(2gt)\exp\left(-\frac{t^2}{\tau_C^2}\right), \qquad (5.38)$$

with τ_C being the collapse time, given by $\tau_C = \sqrt{2}/g$. For an atom initially in $|g\rangle$ the result is

$$\rho_{11}(t) = \frac{1}{2} - \frac{1}{2}\cos(2gt)\exp\left(-\frac{t^2}{\tau_C^2}\right). \qquad (5.39)$$

Therefore, after the collapse the diagonal elements are constant, and $\rho_{ii} = 1/2$.

The off-diagonal element ρ_{01} (again, first for the atom initially in $|e\rangle$) is given by

$$\rho_{01}(t) = \sum_n \langle \psi_e(t)|n, g\rangle \langle n, e|\psi_e(t)\rangle. \qquad (5.40)$$

Evaluating the summands $\rho_{01}^{(n)}$ using Eq. (5.37) and Eq. (5.28) leads to

$$\rho_{01}^{(n)}(t) = iw(n)\frac{\sqrt{n}}{2\alpha^*}e^{-i\omega t}\left\{ \sin\left[(\Omega_{n+1} + \Omega_n)\frac{t}{2}\right] - \sin\left[(\Omega_{n+1} - \Omega_n)\frac{t}{2}\right] \right\}, \qquad (5.41)$$

with $w(n)$ being the Poisson distribution. The first term inside the square brackets oscillates at a much higher frequency than the second and results only in a random phase, which vanishes after summation. In the high-photon limit $\sqrt{n}$ may be approximated by (see [Gea-Banacloche90])

$$\sqrt{n} \approx \sqrt{\bar{n}} + \frac{n - \bar{n}}{2\sqrt{\bar{n}}}. \qquad (5.42)$$

Analogously, the difference of the Rabi frequencies can be expressed as

$$\Omega_{n+1} - \Omega_n = 2g(\sqrt{n+1} - \sqrt{n}) \qquad (5.43)$$

$$\approx 2g\left(\frac{1}{2\sqrt{\bar{n}}} - \frac{1}{8\sqrt{\bar{n}^3}} - \frac{n - \bar{n}}{4\sqrt{\bar{n}^3}}\right). \qquad (5.44)$$

Plugging only the leading order into Eq. (5.41) and replacing the sum in Eq. (5.40) by an integral over a Gaussian distribution leads to

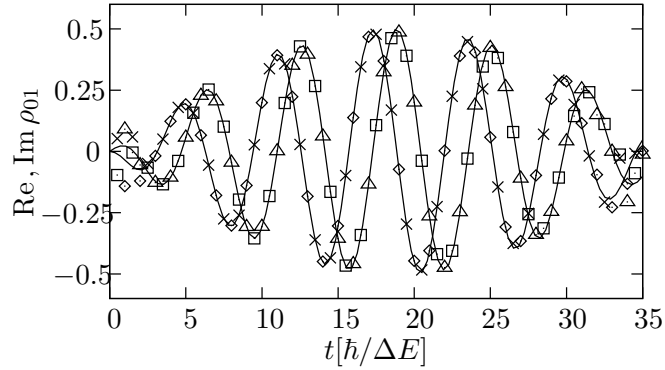$$\rho_{01}(t) = -\frac{i}{2}\exp[i(\omega t + \phi)]\sin\frac{gt}{2\sqrt{\bar{n}}}, \qquad (5.45)$$

Figure 5.4.: Comparison of the real and imaginary part of Eq. (5.45) (solid lines) and the solution of the full time-dependent Schrödinger equation. Initial states for the atom were $|g\rangle$ (Re ρ_{01}: crosses, Im ρ_{01}: boxes) and $|e\rangle$ (Re ρ_{01}: diamonds, Im ρ_{01}: triangles). ($\bar{n} = 36$, $g = 1, \phi = 0$)

where ϕ is the initial phase of the radiation field. Using the same approximations for the atom initially in its ground state yields the same result for $\rho_{01}(t)$. Therefore, after the collapse the atom evolves totally independent from its initial state. A comparison of Eq. (5.45) with the numerical solution of the full time-dependent Schrödinger equation is shown in Fig. 5.4. Apart from the collapse and revival phase there is excellent agreement.

Since the diagonal elements of $\hat{\rho}$ are both at $\frac{1}{2}$ the Bloch vector only moves within $x - -y$ plane of the Bloch sphere. Therefore, in order to obtain a thermal state one always has to apply a $\frac{\pi}{2}$ pulse to the system (see Fig. 5.5), which is independent of the exact position within the $x - -y$ plane. Since the pulse diagonalizes $\hat{\rho}$, the probability to find the atom in its excited state after the pulse $p_e(t)$ is given by the smallest eigenvalue of $\hat{\rho}$. Computation of $p_e(t)$ yields

$$p_e(t) = \frac{1}{2}\left(1 - \sin\frac{gt}{2\sqrt{\bar{n}}}\right). \tag{5.46}$$

This can also be expressed as a temperature using

$$T = -\frac{\Delta E}{k_B \log\left(\frac{p_e}{1-p_e}\right)}. \tag{5.47}$$

5.4. Minimum and maximum temperature

Equation (5.46) suggests that at half of the revival time the atom will be in its ground state (i.e., $T = 0$). However, this minimum temperature would only be reached for infinitely large $\bar{n}$, for which it would take an infinitely long time to reach this state. In order to determine the actual minimum temperature a correction for finite $\bar{n}$ is required.
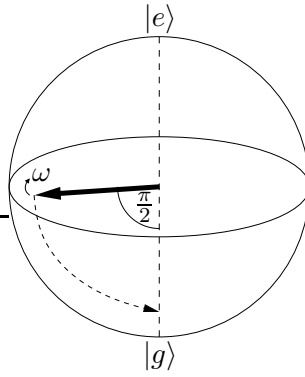
Figure 5.5.: Illustration of the $\frac{\pi}{2}$ pulse acting on the Bloch vector of the atom.
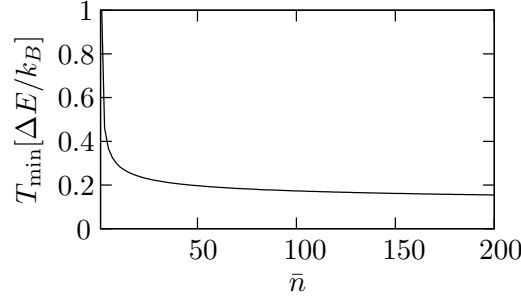

Figure 5.6.: Minimum temperature $T_{\min}$ over average photon number $\bar{n}$.

A correction to Eq. (5.45) can be obtained by including the next order in Eq. (5.44). Close to half of the revival time the sine in Eq. (5.41) is near its maximum and can be approximated by a second order Taylor expansion, which leads to a final result of

$$p_e\left(\frac{\tau_R}{2}\right) = \frac{\pi^2}{32\bar{n}}. \tag{5.48}$$

Using the next order in Eq. (5.42) as well leads to an additional correction in $O(\frac{1}{\bar{n}^2})$. Putting this p_e into Eq. (5.47) gives the minimum temperature $T_{\min}(\bar{n})$ as shown in Fig. 5.6.

In order to determine the maximum temperature that can be reached we require that the collapse must have taken place [i.e,. the difference in the occupation probabilities Eqs. (5.38) and (5.39) is negligible compared to the difference induced by the laser]. Requiring the former to be smaller by a factor of 10, this can be expressed as

$$10\cos(2gt)\exp\left(-\frac{t^2}{\tau_C^2}\right) = \sin\frac{gt}{2\sqrt{\bar{n}}}. \tag{5.49}$$

The cosine on the left hand side may be replaced by unity without violating the above requirement. For large $\bar{n}$ the right hand side can be approximated linearly in t, resulting in

$$10\exp\left(-\frac{t^2}{\tau_C^2}\right) = \frac{gt}{2\sqrt{\bar{n}}}. \tag{5.50}$$
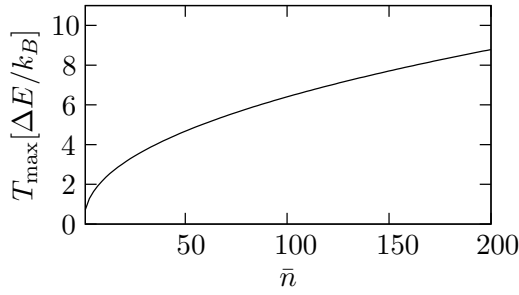
Figure 5.7.: Maximum temperature $T_{\max}$ over average photon number $\bar{n}$.

Solving for the appropriate cavity interaction time t and using Eqs. (5.46) and (5.47) leads to a maximum temperature $T_{\max}$ of

$$T_{\max} = \frac{\Delta E}{k_B \log \frac{4\sqrt{\bar{n}}+\sqrt{W(400\bar{n})}}{4\sqrt{\bar{n}}-\sqrt{W(400\bar{n})}}}, \tag{5.51}$$

where $W(\cdot)$ denotes the Lambert W function, i.e., the inverse function of $f(x) = x\mathrm{e}^x$. Figure 5.7 shows the dependence of $T_{\max}$ on $\bar{n}$.

5.5. Entropy transport

In order to investigate the dynamical properties of the cooling or heating of the atom it is convenient to calculate its von Neumann entropy. Figure 5.8 shows the time-dependence of the entropy for a typical case. In the beginning, the total entropy increases strongly due to the entanglement between atom and field. The amount of entanglement then slowly decreases until it reaches its minimum at half of the revival time. Subsequently, the total entropy increases again. The local entropy of the field rapidly approaches the entropy of the atom. Following this, it remains constant until the revival phase. This means that the rate of entropy transport from the atom to the field is the same as the rate for the total entropy (and thus entanglement) decrease.

5.6. Applications

These results show that the temperature of the atom can be tuned over a large range that depends only on the average photon number $\bar{n}$, the coupling time t, and the energy splitting ΔE. However, there are some other applications for this procedure, which are realizable within present experimental setups. A rather obvious one is the cooling of atoms. However, an implementation using an optical cavity would be extremely difficult as the frequencies relevant for cooling are in the MHz range, where the coupling constant g is much too small to observe any effects [due to the ω dependence in Eq. (5.23)]. A much more promising implementation could be realized using circuit quantum
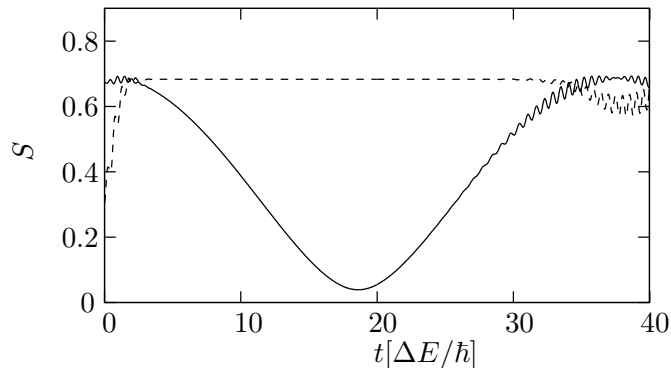
Figure 5.8.: Local entropy for the atom (solid line) and the radiation field (dashed line). $(g = 1,\ \alpha = 6,\ \beta = 2.5\Delta E)$

electrodynamics (QED) [Blais04; Wallraff04], in which the atom is replaced by a Cooper-pair box and the cavity is implemented by a one-dimensional resonator. There, the coupling constant is sufficiently large even in the relevant frequency range. Using our procedure might lead to lower temperatures than resulting from currently employed techniques. Besides circuit QED, other implementations involving a Jaynes-Cummings Hamiltonian with a tunable coupling constant may prove useful as well.

Another interesting application of this procedure could be the realization of tiny local baths. Local baths are an important ingredient in non-equilibrium quantum thermodynamics [Gemmer04], where it is necessary to create and control a temperature gradient on a nanoscopic scale. This could be used to investigate transport behavior [Saito00; Michel03] or quantum thermodynamic machines [Henrich06]. Using our framework to repeatedly set a temperature of a single two-level system could act as such a local bath, as long as the cavity is reset after each step and the temperature control happens on a much smaller timescale than the other processes within the system (i.e., strong bath coupling).

6. Summary and Conclusion

As laid out in the beginning, exponentially growing computational resources are the main obstacle when investigating complex quantum systems. However, the main part of this thesis states that not all is lost. There are classes of quantum systems that are thermodynamic in the sense that it is possible to correctly describe essential properties like transport behavior without having to solve the full time-dependent Schrödinger equation. This even holds far from equilibrium.

In chapter 3, the LEMBAS principle was introduced. While in general it still requires the solution to the full problem, it is possible to use it to find constraints on stationary steady states, thus reducing the search space dramatically. Additionally, definitions for work and heat are much more obvious in the context of the LEMBAS principle. However, the relation to results from classical non-equilibrium thermodynamics, like the principle of minimum entropy production, remains an open problem.

The most powerful approach for tackling large thermodynamic quantum systems is the projection operator technique used in chapter 4. While being a perturbative approach, it can give a good approximation to the dynamics of the system for all times. Using this method, the transport properties of a concrete three-dimensional magnetic system have been investigated. There, diffusive and ballistic heat transport have been found to coexist in the same system, depending only oon the direction the transport is being invenstigated. Furthermore, diffusive behavior has been found to be an emergent property, as it does not exist on the scale of a single spin, but only when a reasonably large amount of spins is considered.

Finally, chapter 5 demonstrates that quantum thermodynamics can directly lead to useful applications: Using a straightforward setup it is possible to control the temperature of a two-level system. This scenario could be used in any case where extremely cooled internal degrees of freedom are desirable, like in quantum computing or even for medical applications such as magnetic resonance imaging.

In summary, this thesis demonstrates that transport properties of quantum system can be studied using standard techniques. The methods are not limited to classical concepts like work and heat, but are also applicable in a more general sense for quantities like entropy and entanglement.

6. Summary and Conclusion

A. Appendix

A.1. Trace theorems

Let $\mathcal{H} = \mathcal{H}_A \otimes \mathcal{H}_B$ be a bipartite Hilbert space, with operators $\hat{A}$ and $\hat{B}$ acting on $\mathcal{H}_1$ and $\mathcal{H}_2$, respectively, and an operator $\hat{C}$ acting on the full Hilbert space.

Theorem A.1.

$$\text{Tr}_A \left\{ [\hat{A} \otimes \hat{1}, \hat{C}] \right\} = \text{Tr}_B \left\{ [\hat{1} \otimes \hat{B}, \hat{C}] \right\} = 0.$$

Proof. Due to symmetry it suffices to prove

$$\text{Tr}_A \left\{ [\hat{A} \otimes \hat{1}, \hat{C}] \right\} = 0. \tag{A.1}$$

Using an orthonormal basis $\{\hat{Q}_i\}$ with each $\hat{Q}_i$ acting only on $\mathcal{H}_A$ or $\mathcal{H}_B$ we can write

$$
\begin{aligned}
\text{Tr}_A \left\{ [\hat{A} \otimes \hat{1}, \hat{C}] \right\} &= \sum_{jk} c_{jk} \text{Tr}_A \left\{ [\hat{A} \otimes \hat{1}, \hat{Q}_j \otimes \hat{Q}_k] \right\} \\
&= \sum_{jk} c_{jk} \text{Tr}_A \left\{ [\hat{A} \otimes \hat{1}, \hat{Q}_j] \otimes \hat{Q}_k \right\} \\
&= \sum_{jk} c_{jk} \text{Tr}_A \left\{ [\hat{A}, \hat{Q}_j] \right\} \hat{Q}_k \\
&\overset{cycl.}{=} 0. \tag{A.2}
\end{aligned}
$$

$\square$

Theorem A.2.

$$
\begin{aligned}
\text{Tr}_A \left\{ (\hat{A} \otimes \hat{B})\hat{C} \right\} &= \hat{B} \text{Tr}_A \left\{ (\hat{A} \otimes \hat{1})\hat{C} \right\} \\
\text{Tr}_B \left\{ (\hat{A} \otimes \hat{B})\hat{C} \right\} &= \hat{A} \text{Tr}_B \left\{ (\hat{1} \otimes \hat{B})\hat{C} \right\}.
\end{aligned}
$$

Proof. Again, for symmetry reasons we only need to prove the first part. Using the same

basis operators as in the proof of theorem A.1 we have

$$
\begin{aligned}
\mathrm{Tr}_A\left\{(\hat{A}\otimes\hat{B})\hat{C}\right\} &= \sum_{jk} c_{jk}\mathrm{Tr}_A\left\{(\hat{A}\otimes\hat{B})(\hat{Q}_j\otimes\hat{Q}_k)\right\} \\
&= \sum_{jk} c_{jk}\mathrm{Tr}_A\left\{(\hat{A}\hat{Q}_j)\otimes(\hat{B}\hat{Q}_k)\right\} \\
&= \hat{B}\sum_{jk} c_{jk}\mathrm{Tr}_A\left\{(\hat{A}\hat{Q}_j)\otimes\hat{Q}_k\right\} \\
&= \hat{B}\mathrm{Tr}_A\left\{(\hat{A}\otimes\hat{1})\hat{C}\right\}.
\end{aligned}
\tag{A.3}
$$

$\square$

Corollary A.3. *If the operator acting on the system being traced out is the unit operator, it immediately follows from theorem A.2 that*

$$
\begin{aligned}
\mathrm{Tr}_A\left\{(\hat{1}\otimes\hat{B})\hat{C}\right\} &= \hat{B}\mathrm{Tr}_A\left\{\hat{C}\right\} \\
\mathrm{Tr}_B\left\{(\hat{A}\otimes\hat{1})\hat{C}\right\} &= \hat{A}\mathrm{Tr}_B\left\{\hat{C}\right\}.
\end{aligned}
\tag{A.4}
$$

Corollary A.4. *Another immediate consequence of theorem A.2 is*

$$
\begin{aligned}
\mathrm{Tr}_B\left\{\left[\hat{C},\hat{A}\otimes\hat{B}\right]\right\} &= \left[\mathrm{Tr}_B\left\{\hat{C}(\hat{1}\otimes\hat{B})\right\},\hat{A}\right] \\
\mathrm{Tr}_A\left\{\left[\hat{C},\hat{A}\otimes\hat{B}\right]\right\} &= \left[\mathrm{Tr}_A\left\{\hat{C}(\hat{A}\otimes\hat{1})\right\},\hat{B}\right].
\end{aligned}
\tag{A.5}
$$

A.2. Reduced density matrices

Theorem A.5. *Let $\mathcal{H} = \mathcal{H}_A \otimes \mathcal{H}_B$ be a bipartite Hilbert space. We may write any density operator $\hat{\rho}$ as*

$$
\hat{\rho} = \hat{\rho}_A \otimes \hat{\rho}_B + \hat{C}_{AB},
\tag{A.6}
$$

with $\hat{\rho}_{A,B}$ being the reduced density matrices of subsystem A, B, respectively, and $\hat{C}_{AB}$ being the operator representing the correlations (both classical correlations and entanglement). Then

$$
\mathrm{Tr}_A\left\{\hat{C}_{AB}\right\} = \mathrm{Tr}_B\left\{\hat{C}_{AB}\right\} = 0.
\tag{A.7}
$$

Proof. As discussed above, we only need to prove the first part. Taking the partial trace over A results in

$$
\begin{aligned}
\mathrm{Tr}_A\left\{\hat{\rho}\right\} &= \mathrm{Tr}_A\left\{\hat{\rho}_A\otimes\hat{\rho}_B\right\} + \mathrm{Tr}_A\left\{\hat{C}_{AB}\right\} \\
\hat{\rho}_A &= \hat{\rho}_A + \mathrm{Tr}_A\left\{\hat{C}_{AB}\right\} \\
\mathrm{Tr}_A\left\{\hat{C}_{AB}\right\} &= 0.
\end{aligned}
\tag{A.8}
$$

$\square$

Corollary A.6. *By taking the trace over the remaining system in theorem A.5 we arrive at*

$$\text{Tr}\left\{C_{AB}\right\} = 0. \tag{A.9}$$

A. Appendix

Bibliography

[Alicki79]   R. Alicki. The quantum open system as a model of the heat engine. *J. Phys. A*, **12**, L103 (1979).

[Araki70]   H. Araki and E. H. Lieb. Entropy inequalities. *Comm. Math. Phys.*, **18**, 160 (1970).

[Ballentine98]   L. E. Ballentine. *Quantum Mechanics* (World Scientific, Singapore, 1998).

[Basdevant00]   J.-L. Basdevant and J. Dalibard. *The Quantum Mechanics Solver* (Springer, Berlin, 2000).

[Bjorken65]   J. D. Bjorken and S. D. Drell. *Relativistic quantum fields* (McGraw-Hill,, New York, 1965).

[Blais04]   A. Blais, R.-S. Huang, A. Wallraff, S. M. Girvin, and R. J. Schoelkopf. Cavity quantum electrodynamics for superconducting electrical circuits: An architecture for quantum computation. *Phys. Rev. A*, **69**, 062320 (2004).

[Blank94]   J. Blank, P. Exner, and M. Havlícek. *Hilbert space operators in quantum physics* (AIP, New York, 1994).

[Borowski03]   P. Borowski, J. Gemmer, and G. Mahler. Relaxation to equilibrium under pure Schrödinger dynamic. *Euro. Phys. J. B*, **31**, 249 (2003).

[Breuer02]   H.-P. Breuer and F. Petruccione. *The Theory of Open Quantum Systems* (Oxford University Press, Oxford, 2002).

[Breuer06]   H.-P. Breuer, J. Gemmer, and M. Michel. Non-Markovian quantum dynamics: Correlated projection superoperators and Hilbert space averaging. *Phys. Rev. E*, **73**, 016139 (2006).

[Breuer07]   H.-P. Breuer. Non-Markovian generalization of the Lindblad theory of open quantum systems. *Phys. Rev. A*, **75**, 022103 (2007).

[Brune96]   M. Brune, F. Schmidt-Kaler, A. Maali, J. Dreyer, E. Hagley, J. M. Raimond, and S. Haroche. Quantum Rabi Oscillation: A Direct Test of Field Quantization in a Cavity. *Phys. Rev. Lett.*, **76**, 1800 (1996).

Bibliography

[Chu98]   S. Chu. Nobel Lecture: The manipulation of neutral particles. *Rev. Mod. Phys.*, **70**, 685 (1998).

[Cohen-Tannoudji77]   C. Cohen-Tannoudji, B. Diu, and F. Laloë. *Quantum mechanics* (Wiley, New York, 1977).

[Cohen-Tannoudji98]   C. N. Cohen-Tannoudji. Nobel Lecture: Manipulating atoms with photons. *Rev. Mod. Phys.*, **70**, 707 (1998).

[Delamotte04]   B. Delamotte. A hint of renormalization. *American Journal of Physics*, **72**, 170 (2004).

[DiVincenzo00]   D. P. DiVincenzo. The Physical Implementation of Quantum Computation. *Fortschr. Phys.*, **48**, 771 (2000).

[Gea-Banacloche90]   J. Gea-Banacloche. Collapse and revival of the state vector in the Jaynes-Cummings model: An example of state preparation by a quantum apparatus. *Phys. Rev. Lett.*, **65**, 3385 (1990).

[Gemmer01a]   J. Gemmer and G. Mahler. Entanglement and the factorization-approximation. *Eur. Phys. J. D*, **17**, 385 (2001).

[Gemmer01b]   J. Gemmer, A. Otte, and G. Mahler. Quantum Approach to a Derivation of the Second Law of Thermodynamics. *Phys. Rev. Lett.*, **86**, 1927 (2001).

[Gemmer03]   J. Gemmer and G. Mahler. Distribution of local entropy in the Hilbertspace of bi-partite qauntum systems: Origin of Jaynes' principle. *Europyhs. Lett.*, **62**, 629 (2003).

[Gemmer04]   J. Gemmer, M. Michel, and G. Mahler. *Quantum Thermodynamics*. Lecture Notes in Physics, Vol. 657 (Springer, Berlin, 2004).

[Gemmer06]   J. Gemmer, R. Steinigeweg, and M. Michel. Limited validity of the Kubo formula for thermal conduction in modular quantum systems. *Phys. Rev. B*, **73**, 104302 (2006).

[Gobert05]   D. Gobert, C. Kollath, U. Schollwöck, and G. Schütz. Real-time dynamics in spin-(1/2) chains with adaptive time-dependent density matrix renormalization group. *Phys. Rev. E*, **71**, 036102 (2005).

[Hartmann04a]   M. Hartmann, G. Mahler, and O. Hess. Existence of Temperature on the Nanoscale. *Phys. Rev. Lett.*, **93**, 080402 (2004).

[Hartmann04b]   M. Hartmann, G. Mahler, and O. Hess. Local Versus Global Thermal States: Correlations and the Existence of Local Temperatures. *Phys. Rev. E*, **70**, 066148 (2004).

[Heidrich-Meisner03] F. Heidrich-Meisner, A. Honecker, D. C. Cabra, and W. Brenig. Zero-frequency transport properties of one-dimensional spin-(1/2) systems. *Phys. Rev. B*, **68**, 134436 (2003).

[Henrich06] M. J. Henrich, M. Michel, and G. Mahler. Small quantum networks operating as quantum thermodynamic machines. *Europhys. Lett.*, **76**, 1057 (2006).

[Hess01] C. Hess, C. Baumann, U. Ammerahl, B. Büchner, F. Heidrich-Meisner, W. Brenig, and A. Revcolevschi. Magnon heat transport in $(Sr, Ca, La)_{14}Cu_{24}O_{41}$. *Phys. Rev. B*, **64**, 184305 (2001).

[Jaynes63] E. T. Jaynes and F. W. Cummings. Comparison of quantum and semiclassical radiation theories with application to the beam maser. *Proc. IEEE*, **51**, 89 (1963).

[Jung06] P. Jung, R. W. Helmes, and A. Rosch. Transport in Almost Integrable Models: Perturbed Heisenberg Chains. *Phys. Rev. Lett.*, **96**, 067202 (2006).

[Kieu04] T. D. Kieu. The Second Law, Maxwell's Demon, and Work Derivable from Quantum Heat Engines. *Phys. Rev. Lett.*, **93**, 140403 (2004).

[Klümper02] A. Klümper and K. Sakai. The thermal conductivity of the spin-1/2 XXZ chain at arbitrary temperature. *J. Phys. A*, **35**, 2173 (2002).

[Kosloff84] R. Kosloff and M. A. Ratner. Beyond linear response: Line shapes for coupled spins or oscillators vi a direct calculation of dissipated power. *J. of Chem. Phys.*, **80**, 2352 (1984).

[Kubo57] R. Kubo. Statistical-Mechanical Theory of Irreversible Processes. I. *J. Phys. Soc. Jpn.*, **12**, 570 (1957).

[Kubo91] R. Kubo, M. Toda, and N. Hashitsume. *Statistical Physics II: Nonequilibrium Statistical Mechanics.* Number 31 in Solid-State Sciences, 2. edition (Springer, Berlin, Heidelberg, New-York, 1991).

[Luttinger64] J. M. Luttinger. Theory of Thermal Transport Coefficients. *Phys. Rev.*, **135**, A1505 (1964).

[Mehta91] M. L. Mehta. *Random Matrices* (Academic Press, Boston, 1991).

[Mejía-Monasterio05] C. Mejía-Monasterio, T. Prosen, and G. Casati. Fourier's law in a quantum spin chain and the onset of quantum chaos. *Europhys. Lett.*, **72**, 520 (2005).

[Michel03] M. Michel, M. Hartmann, J. Gemmer, and G. Mahler. Fourier's Law confirmed for a class of small quantum systems. *Eur. Phys. J. B*, **34**, 325 (2003).

[Michel04] M. Michel, J. Gemmer, and G. Mahler. Heat conductivity in small quantum systems: Kubo formula in Liouville space. *Eur. Phys. J. B*, **42**, 555 (2004).

[Michel05] M. Michel, G. Mahler, and J. Gemmer. Fourier's Law from Schr[o-umlaut]dinger Dynamics. *Phys. Rev. Lett.*, **95**, 180602 (2005).

[Michel06] M. Michel, J. Gemmer, and G. Mahler. Application of the Hilbert space average method on heat conduction models. *Phys. Rev. E*, **73**, 016101 (2006).

[Nakajima58] S. Nakajima. On Quantum Theory of Transport Phenomena – Steady Diffusion. *Progr. Theo. Phys.*, **20**, 948 (1958).

[Phillips98] W. D. Phillips. Nobel Lecture: Laser cooling and trapping of neutral atoms. *Rev. Mod. Phys.*, **70**, 721 (1998).

[Phoenix91] S. J. D. Phoenix and P. L. Knight. Establishment of an entangled atom-field state in the Jaynes-Cummings model. *Phys. Rev. A*, **44**, 6023 (1991).

[Prigogine67] I. Prigogine. *Introduction to thermodynamics of irreversible processes* (Interscience, New York, 1967).

[Rempe87] G. Rempe, H. Walther, and N. Klein. Observation of quantum collapse and revival in a one-atom maser. *Phys. Rev. Lett.*, **58**, 353 (1987).

[Saito00] K. Saito, S. Takesue, and S. Miyashita. Energy transport in the integrable system in contact with various types of phonon reservoirs. *Phys. Rev. E*, **61**, 2397 (2000).

[Saito03] K. Saito. Transport anomaly in the low-energy regime of spin chains. *Phys. Rev. B*, **67**, 064410 (2003).

[Satyanarayana92] M. V. Satyanarayana, M. Vijayakumar, and P. Alsing. Glauber-Lachs version of the Jaynes-Cummings interaction of a two-level atom. *Phys. Rev. A*, **45**, 5301 (1992).

[Schollwöck04] U. Schollwöck, J. Richter, D. J. Farnell, and R. F. Bishop (Editors). *Quantum Magnetism*. Lecture Notes in Physics, Vol. 645 (Springer, Berlin, 2004).

[Schwabl98] F. Schwabl. *Quantenmechanik* (Springer, Berlin, 1998).

[Schwabl00] F. Schwabl. *Statistische Mechanik* (Springer, Berlin, 2000).

[Shibata77] F. Shibata, Y. Takahashi, and N. Hashitsume. A generalized stochastic liouville equation. Non-Markovian versus memoryless master equations. *J. Stat. Phys.*, **17**, 171 (1977).

[Shore93] B. W. Shore and P. L. Knight. The Jaynes-Cummings Model. *J. Mod. Opt.*, **40**, 1195 (1993).

[Sologubenko00] A. V. Sologubenko, K. Giannó, H. R. Ott, U. Ammerahl, and A. Revcolevschi. Thermal Conductivity of the Hole-Doped Spin Ladder System $Sr_{14-x}Ca_xCu_{24}O_{41}$. *Phys. Rev. Lett.*, **84**, 2714 (2000).

[Steinigeweg06] R. Steinigeweg, J. Gemmer, and M. Michel. Normal-transport behavior in finite one-dimensional chaotic quantum systems. *Europhys. Lett.*, **75**, 406 (2006).

[Wallraff04] A. Wallraff, D. I. Schuster, A. Blais, L. Frunzio, R. S. Huang, J. Majer, S. Kumar, S. M. Girvin, and R. J. Schoelkopf. Circuit Quantum Electrodynamics: Coherent Coupling of a Single Photon to a Cooper Pair Box. *Nature*, **431**, 162 (2004).

[Walls94] D. F. Walls and G. J. Milburn. *Quantum Optics* (Springer, Berlin, 1994).

[Weimer07] H. Weimer, M. Henrich, F. Rempp, H. Schröder, and G. Mahler. Local effective dynamics of quantum systems: work and heat. *in preparation* (2007).

[Wichterich07] H. Wichterich, M. J. Henrich, H.-P. Breuer, J. Gemmer, and M. Michel. Modeling heat transport through completely positive maps. *quant-ph/0703048* (2007).

[Yoo85] H.-I. Yoo and J. H. Eberly. Dynamical theory of an atom with two or three levels interacting with quantized cavity fields. *Phys. Rep.*, **118**, 239 (1985).

[Zotos97] X. Zotos, F. Naef, and P. Prelovsek. Transport and conservation laws. *Phys. Rev. B*, **55**, 11029 (1997).

[Zurek05] W. H. Zurek. Probabilities from entanglement, Born's rule $p_k = |\psi_k|^2$ from envariance. *Phys. Rev. A*, **71**, 052105 (2005).

[Zwanzig60] R. Zwanzig. Ensemble Method in the Theory of Irreversibility. *J. Chem. Phys.*, **33**, 1338 (1960).

Acknowledgements